AD-A069 484 KING (WILLIAM R) ALEXANDRIA VA F/G 9/5
STABLE MESA ANTENNA PATTERNS.(U)
MAY 79 W R KING
UNCLASSIFIED NRL-MR-3998 N00014-78-C-0681 NL

1 OF 1
AD
A069484

END
DATE FILMED
7-79
DDC

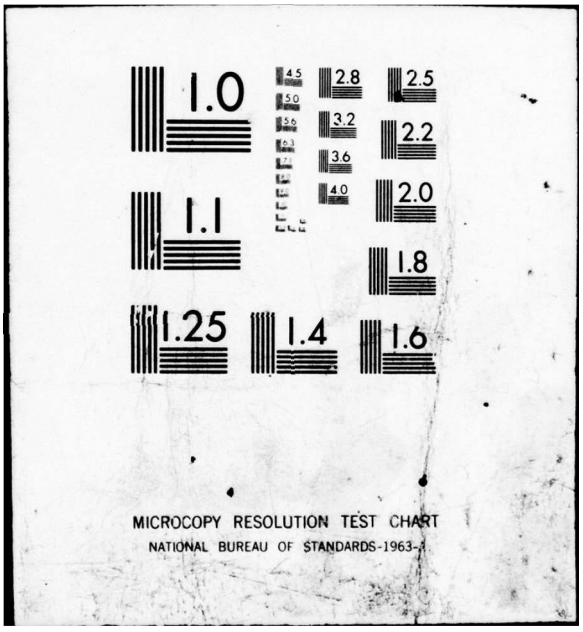
1.0
1.1
1.25
1.4
1.6
1.8
2.0
2.2
2.5
2.8
3.2
3.6
4.0
4.5
5.0
5.6
MICROCOPY RESOLUTION TEST CHART
NATIONAL BUREAU OF STANDARDS-1963-A

(12) LEVEL II

NRL Memorandum Report 3998

Stable MESA Antenna Patterns

WILLIAM R. KING

Antenna Systems Staff
Radar Division

May 18, 1979

Prepared for the Office of Naval Research Arlington, Virginia 22217
Contract N00014-78-C-0681

NAVAL RESEARCH LABORATORY
Washington, D.C.

SECURITY CLASSIFICATION OF THIS PAGE (When Data Entered)

REPORT DOCUMENTATION PAGE

READ INSTRUCTIONS BEFORE COMPLETING FORM

1. REPORT NUMBER: NRL Memorandum Report 3998	2. GOVT ACCESSION NO. NRL MR-	3. RECIPIENT'S CATALOG NUMBER: 3998
4. TITLE (and Subtitle): STABLE MESA ANTENNA PATTERNS.		5. TYPE OF REPORT & PERIOD COVERED: Interim report on a continuing NRL problem.
		6. PERFORMING ORG. REPORT NUMBER
7. AUTHOR(s): William R. King* (William R.) alex. Va		8. CONTRACT OR GRANT NUMBER(s): Contract N00014-78-C-0681
9. PERFORMING ORGANIZATION NAME AND ADDRESS: Naval Research Laboratory, Washington, DC 20375		10. PROGRAM ELEMENT, PROJECT, TASK AREA & WORK UNIT NUMBERS: 61153N; RR021-05-41; NRL Problem R12-46
11. CONTROLLING OFFICE NAME AND ADDRESS: Office of Naval Research, Arlington, VA 22217		12. REPORT DATE: May 1979
		13. NUMBER OF PAGES: 42
14. MONITORING AGENCY NAME & ADDRESS (If different from Controlling Office)		15. SECURITY CLASS. (of this report): UNCLASSIFIED
		15a. DECLASSIFICATION/DOWNGRADING SCHEDULE

16. DISTRIBUTION STATEMENT (of this Report)

Approved for public release; distribution unlimited.

17. DISTRIBUTION STATEMENT (of the abstract entered in Block 20, if different from Report)

18. SUPPLEMENTARY NOTES

*Present address: 2404 Cameron Mills Road, Alexandria, VA 22302

19. KEY WORDS (Continue on reverse side if necessary and identify by block number)

Maximum entropy
Spectral analysis
Superresolution
Direction finding
Radio emitter location

20. ABSTRACT (Continue on reverse side if necessary and identify by block number)

The maximum entropy spectral analysis (MESA) technique is examined for use in computing spatial antenna patterns. The problem of split peaks is investigated, and five possible stabilization methods are examined. MESA is applied to data simulated for an 8 element antenna linear array.

Split peaks are attributed to interference of noise peaks located in the vicinity of the incident signal. The split peak problem is alleviated with use of the proposed stabilization methods.

Results of the investigation indicate that two of the examined averaging techniques provide excellent stabilization for MESA. Antenna patterns, computed with MESA and either of the

(Continues)

20. Abstract (Continued)

two averaging methods, contain nearly white noise and substantially enhanced SNR.

TABLE OF CONTENTS

STABLE MESA ANTENNA PATTERNS

I. INTRODUCTION

A. Wavenumber Power Spectra

Power spectral analysis techniques are applicable to the processing of spatial multi-channel antenna data, since computed antenna patterns are actually wavenumber power spectra, P(k). The wavenumber k is a function of θ, the signal angle of incidence to the antenna as follows:

$$k = (2\pi/\lambda)\text{SIN}(\theta)$$

Because an antenna array is a collector of spatially sampled data, any power spectral technique which is designed for such discrete data sets is applicable for computing antenna patterns.

B. High Resolution Power Spectral Techniques

During recent years several high resolution power spectral techniques have been developed (or rediscovered) for use with discrete data sets. Some of the techniques are: the maximum entropy method (1), the autoregressive model (2), the moving average model (3), the Yule-Walker technique (4), and the maximum liklihood method (5). Of these techniques the maximum entropy, autoregressive, and Yule-Walker techniques are all pole models, the moving average technique is an all zero model, and maxiumum liklihood is only a criteria function applicable to any model. Most of these methods are described in a tutoral review article (6). These particular methods have also been investigated and compared in two reports (7), (8) in which the best results were achieved with the maximum entropy method.

More conventional high resolution Fourier methods have also been recently developed (9), (10), (11), but have not been so thoroughly investigated. As a consequence, in this paper several methods are investigated for applying the maximum entropy spectral

Note: Manuscript submitted March 15, 1979.

analysis technique (MESA) to the processing of spatial, uniformly sampled data.

C. Application of MESA

Several methods of applying MESA to spatial data are investigated. In particular spatial data, which is simulated for an 8 element linear antenna array, is processed with MESA and the Burg technique (1). The Burg technique is a recursive method for evaluating the MESA filter weights, which substantially reduces the number of calculations required of the more conventional inverse matrix evaluation method.

MESA antenna patterns (wavenumber spectra) may be computed upon the collection of the set of 8 spatial data samples at any instant of time. Such "snapshot" patterns are inherently inconsistent and unstable. However it is possible to compute stable MESA antenna patterns using one of several stablization techniques. It remains only to determine which technique provides sufficient stability for an acceptable averaging period without destroying the desired high resolution property which is characteristic of MESA. Averaging techniques which are investigated employ a time average of one of the follwoing sets of variables:

a.) filter weights
b.) prediction errors
c.) covariance matrix
d.) "snapshot" patterns

And as an alternative to averaging, stablization may also be achieved with use of time adaptive filter weights. In particular a set of adaptive filter weights, which are defined as proportional to the prediction error (12), are utilized in conjunction with a proportionality constant (convergence parameter) to comprise a stable, adaptive MESA processing technique.

II. THE MAXIMUM ENTROPY METHOD

The MESA technique, as the name implies, originated (1) by

maximizing the entropy of a signal mixed with noise. However, the same filter weights may also be derived (13) by whitening the Weiner prediction error filter as specified for discreet data samples (14). The resulting maximum entropy wavenumber spectra P(k) is given as follows:

$$P(k) = \frac{P_N}{\left| 1 + \sum_{n=1}^{N} \gamma_n^N \exp(ikn\Delta x) \right|^2} \qquad (1)$$

where

N = number of filter weights ($1 \leq N \leq M$)
M = number of data samples
P_N = total noise power
ΔX = antenna element spacing
γ_n^N = nth prediction error filter weight of a set of N weights.

The variables of eqn. (1), which are computed using a set of equations known as the "Burg technique", are listed as follows:

a.) Total Noise Power P_N

$P_1 = r_o$ (r_o is the data set autocorrelation function)

$$P_{n+1} = P_n \left[1 + (\gamma_{n+1}^{n+1})^2 \right] \quad \text{for } (1 \leq n \leq N) \qquad (2)$$

b.) Filter Weights γ_n^{N+1}

$$\gamma_1^{N+1} = 1.0$$

$$\gamma_n^{N+1} = \gamma_n^N + \gamma_{N+1}^{N+1} (\gamma_{N-n+2}^N)^* \quad \text{for } (2 \leq n \leq N) \qquad (3)$$

$$\gamma_{N+1}^{N+1} = \frac{-2 \sum_{n=1}^{M-N} (B_n^N)^* \cdot F_{N+n}^N}{\sum_{n=1}^{M-N} \left[(B_n^N)^2 + (F_{N+n}^N)^2 \right]} \qquad \text{for } (1 \le N \le M-1) \qquad (4)$$

c.) Forward Prediction Error F_n^N

$$F_{K+1}^1 = X_{K+1} \qquad \text{for } (1 \le K \le M)$$

$$F_K^{N+1} = \gamma_{N+1}^{N+1} \cdot B_{K-N}^N + F_K^N \qquad \text{for } (N+1 \le K \le M) \qquad (5)$$

d.) Backward Prediction Error B_K^N

$$B_K^1 = X_K \qquad \text{for } (1 \le K \le M-1)$$

$$B_K^{N+1} = (\gamma_{N+1}^{N+1})^* \cdot F_{K+N}^N + B_K^N \qquad \text{for } (1 \le K \le M-N) \qquad (6)$$

where the Kth data sample = X_K for $(1 \le K \le M)$

III. MESA SNAPSHOTS

It is possible to compute an antenna pattern with MESA using only one set of M data samples all recorded at the same instant of time. For example, consider one set of 8 data samples collected with 8 unformly spaced antennas. The Burg technique equations, eqns. (1-6) are initially evaluated for N=1 and M=8, and then evaluated repeatedly for increasing unit incremental values of N up to the desired value of N provided that $(1 \le N \le 7)$.

However the final value of N must be such that ($NS \leq N$) where NS is the number of signals present in the given data set X_K.

Consider a MESA snapshot pattern evaluated for N=4,M=8 where the Burg technique equations are evaluated repeatedly for ($1 \leq N \leq 4$). A MESA snapshot pattern of one signal incident at +10 degrees (0 degrees is broadside to the antenna) and a signal-to-noise ratio of 15 dB is shown in Fig. 1a. The 8 data points contain Guassian, white noise, simulated using a set of 8 random numbers computed for a generator "seed" value of 1 (IR=1). Another MESA snapshot shown in Fig. 1b, is computed using a different set of 8 random numbers for which IR=2.

The single signal is located accurately at +10 degrees (within $\pm$0.5 degrees) in both MESA snapshots of Fig. 1. The side peaks, which are randomly located, occur at different positions in the two snapshots. The total number of peaks, which represent the poles of eqn. (1), is always less or equal to the value of N, the number of filter weights. Since the two independent data sets used in the computed antenna patterns of Fig. 1 are considered to be recorded at two different instances of time, MESA snapshots are clearly time variant when computed with short (M=8) data sets. It is evident that some stablizing technique is needed in the application of MESA to short data sets, so that computed MESA antenna patterns are invariant and repeatable in time for stationary data.

IV. MESA INSTABILITIES

Besides the side peak location instability depicted by Fig. 1, another instability associated with MESA is the inaccurate representation of signal peaks. Signal peaks may not be accurately located at very low signal-to-noise ratios or when other signals are present at adjacent angles. Nearby signals cause distortion in both signal location and in relative signal peak height. It has been noted (15) that isolated MESA signal peaks are not linearly related to the signal-to-noise ratios, but the actual relationship

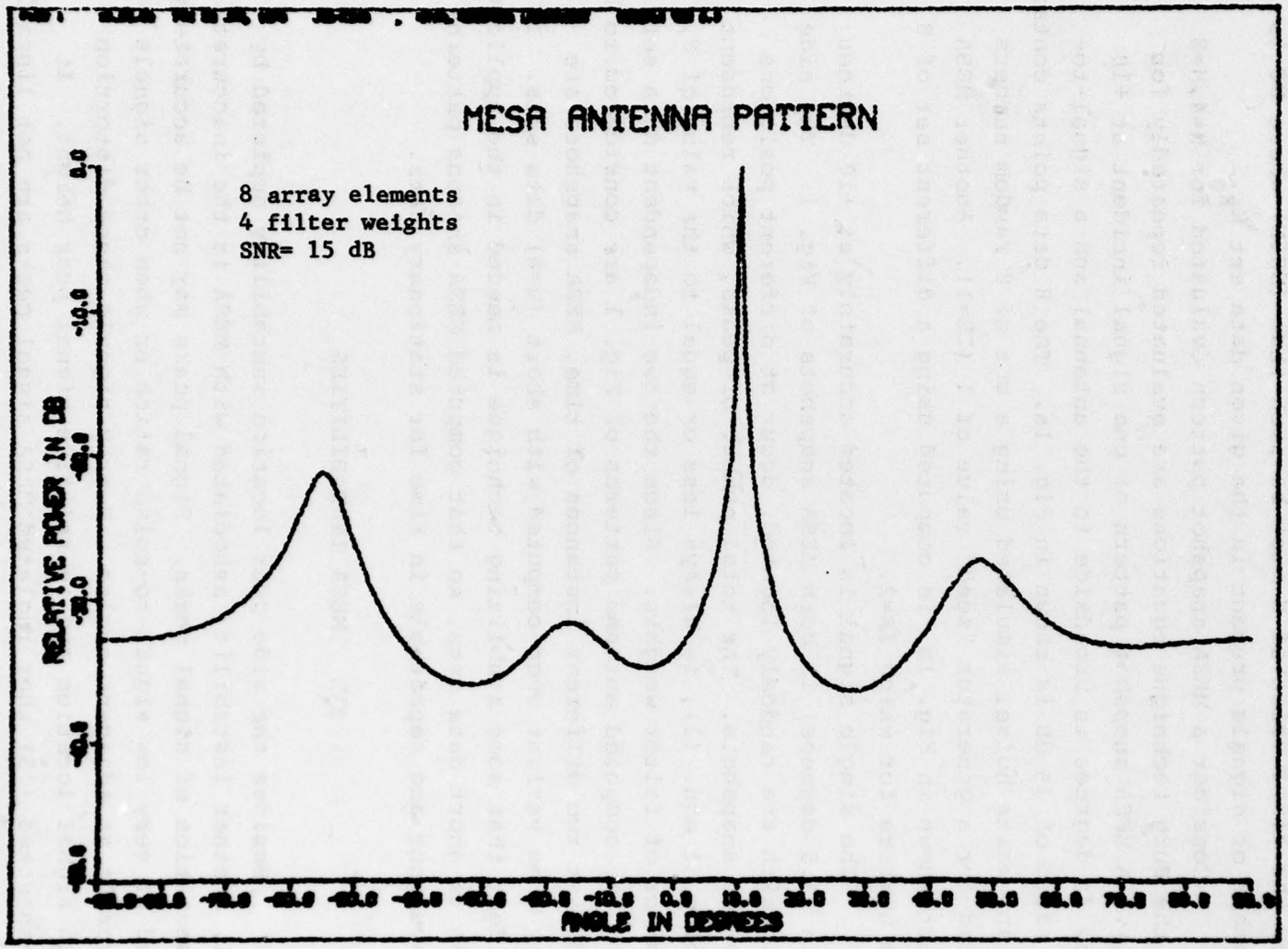

Fig. 1a - MESA snapshot, one signal, IR=1

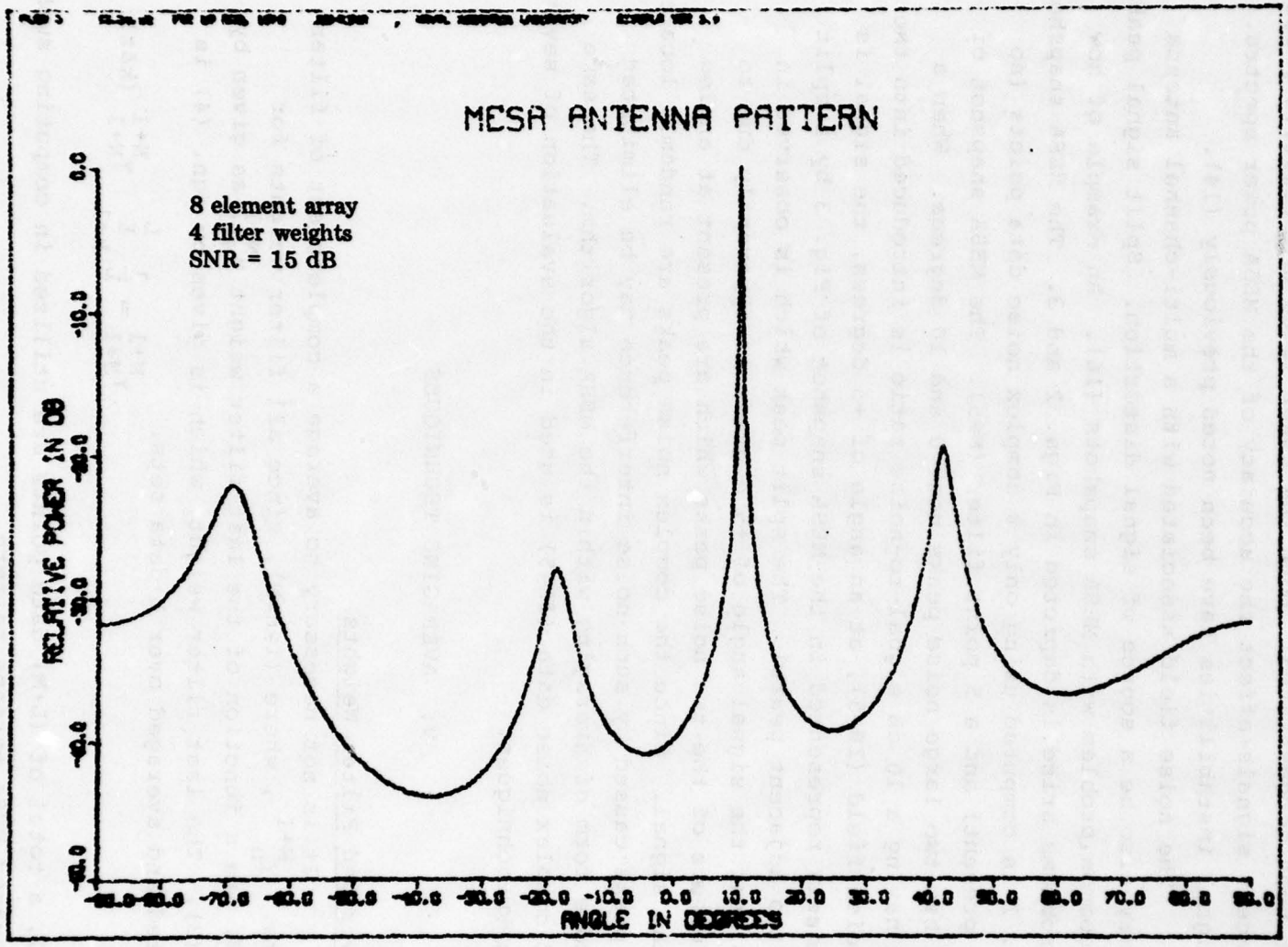

Fig. 1b - MESA snapshot, one signal, IR=2

has not been demonstrated. Both the power level and relative phase of adjacent signals affect the accuracy of the MESA power spectra. Such signal instabilities have been noted previously (14).

The noise field associated with a multi-channel antenna array may also be a source of signal distortion. Split signal peaks are a common problem with MESA snapshots (16). An example of how such problems arise is depicted in Figs. 2 and 3. The MESA snapshot of Fig. 2 is computed using only 8 complex noise data points (no signal present) and a 5 point filter (N=5). The MESA snapshot of Fig. 2 has two large noise peaks near 0 and 10 degrees. When a signal having a 10 dB signal-to-noise ratio is introduced into the same noise field (IR=5), at an angle of +5 degrees, the signal is ambiguously represented in the MESA snapshot of Fig. 3 by a split peak (two adjacent peaks). The split peak which is observed in Fig. 3 near the signal angle of +5 degrees is apparently due to interference of the two noise peaks which are present at angles near the signal. Since the complex noise peaks are randomly located, split peaks caused by such noise interference may be eliminated with some form of averaging within the MESA algorithm. The same set of complex noise data (IR=5) is used in the evaluation of several averaging techniques.

V. AVERAGING TECHNIQUES

A. Averaged Filter Weights

It is not necessary to average a complete set of filter weights. γ_n^{N+1}, where $(1 \leq n \leq N)$, since all filter weights for $(2 \leq n \leq N)$ are a function of the last filter weight γ_{N+1}^{N+1} as given by eqn. (3). The last filter weight, which is given by eqn. (4) is computed and averaged over L data sets.

$$\gamma_{N+1}^{N+1} = \frac{1}{L} \sum_{k=1}^{L} \gamma_{N+1}^{N+1} \; (k\Delta t)$$

In all, a total of (L·M) data points are utilized in computing such an averaged MESA antenna pattern.

An average MESA antenna pattern utilizing an averaged

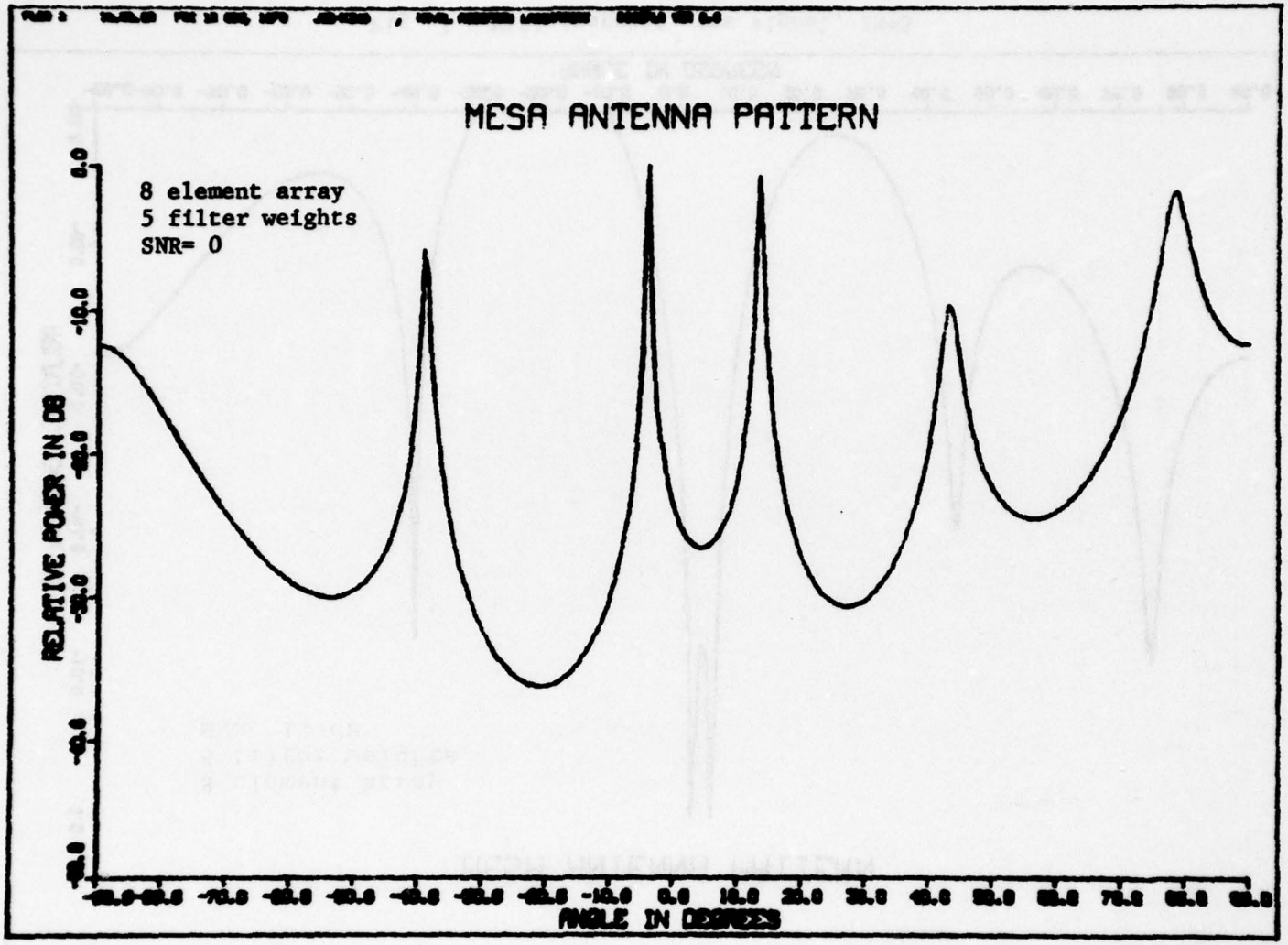

Fig. 2 - MESA snapshot, no signal, IR=5

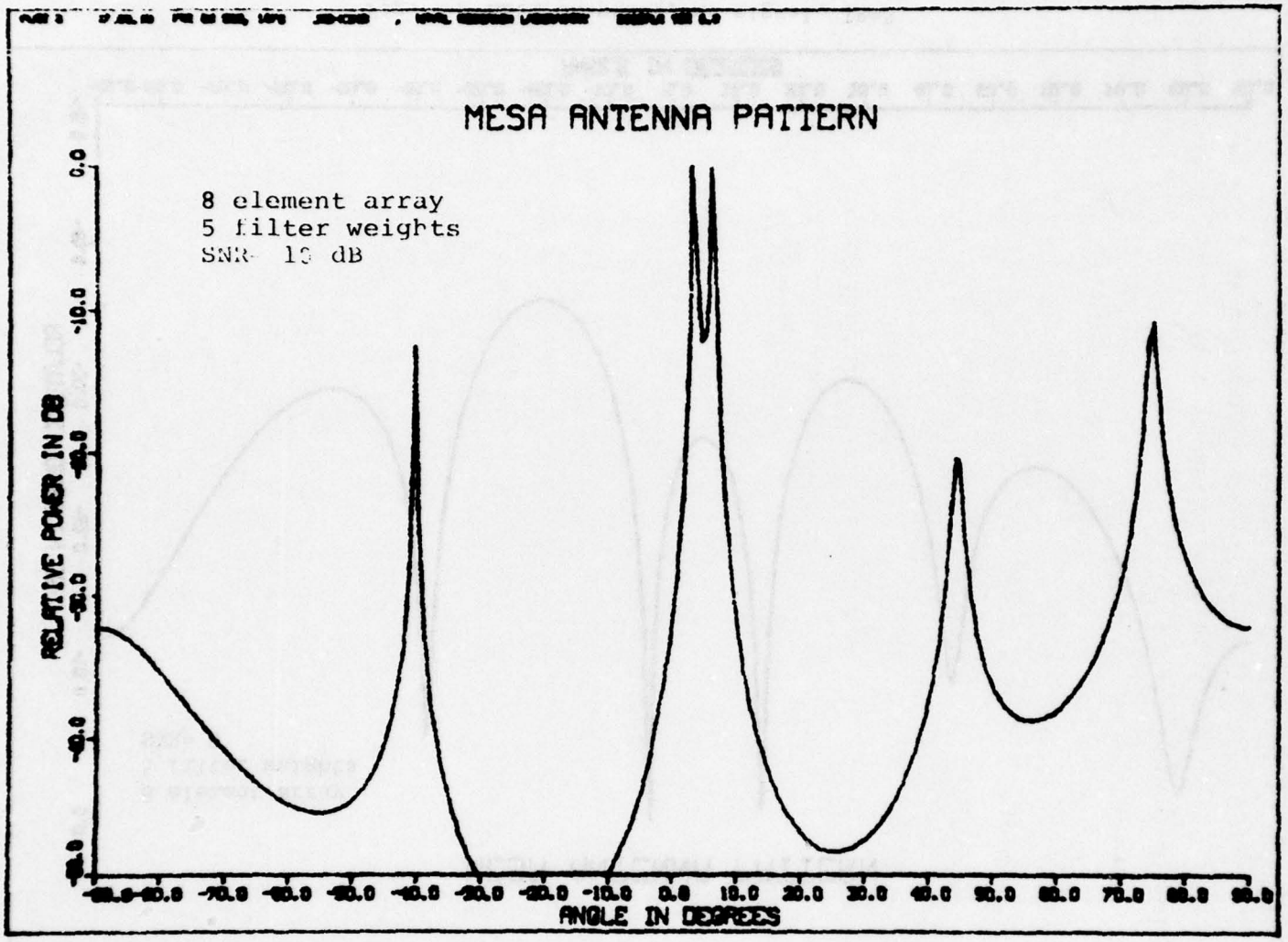

Fig. 3 - MESA snapshot, one signal, IR=5

last filter weight is shown in Fig. 4 for one siganl incident at +5 degrees and a SNR of 10 dB. Peak splitting is eliminated in the example of Fig. 4 with an average of only two filter weights (L=2) and utilizing a total of only 16 data points. The 16 data points include the same complex noise data set used in the example of Fig. 2 (IR=5). The signal is very prominent in the averaged MESA pattern of Fig. 4, although the signal peak is slightly displaced at an angle of +4.5 degrees denoting an inaccuracy of 0.5 degrees. Further averaging beyond L=10 provides little or no improvement. The averaged MESA antenna pattern for L=10, which is shown in Fig. 5, has nearly white noise. The noise peaks are very subdued and are almost eliminated, consequently very little improvement is possible. But the signal peak, which is considerably sharpened, remains at +4.5 degrees with an inaccuracy of 0.5 degrees.

Resolution capability is demonstrated by the averaged MESA antenna pattern of Fig. 6, where two signals with a SNR of 13 dB each signal, each element, are just resolved. Best resolution, which is depicted in Fig. 6, is achieved for N=7 and L=20. The two signals as detected in Fig. 6 are located closer together at angles of 0.5 and 4.5 degrees. The technique of averaging filter weights is a simple and fast stablization technique which results in good resolution and detection capability for a relatively small number of repetitive calculations utilizing 160 (L·M) data points.

B. Averaged Prediction Errors

An averaged MESA antenna pattern may also be computed by averaging the forward and backward prediction errors as defined by eqns. (5) and (6). Prediction errors for filter sizes 1 - N are all calculated in the Burg technique, however best results are achieved by averaging only the set of prediction errors for the specified filter size N as follows:

$$F_n^N = \frac{1}{L} \sum_{k=1}^{L} \left[F_n^N \ (k\Delta t) \right]_k \qquad \text{for } (N \leq n \leq M)$$

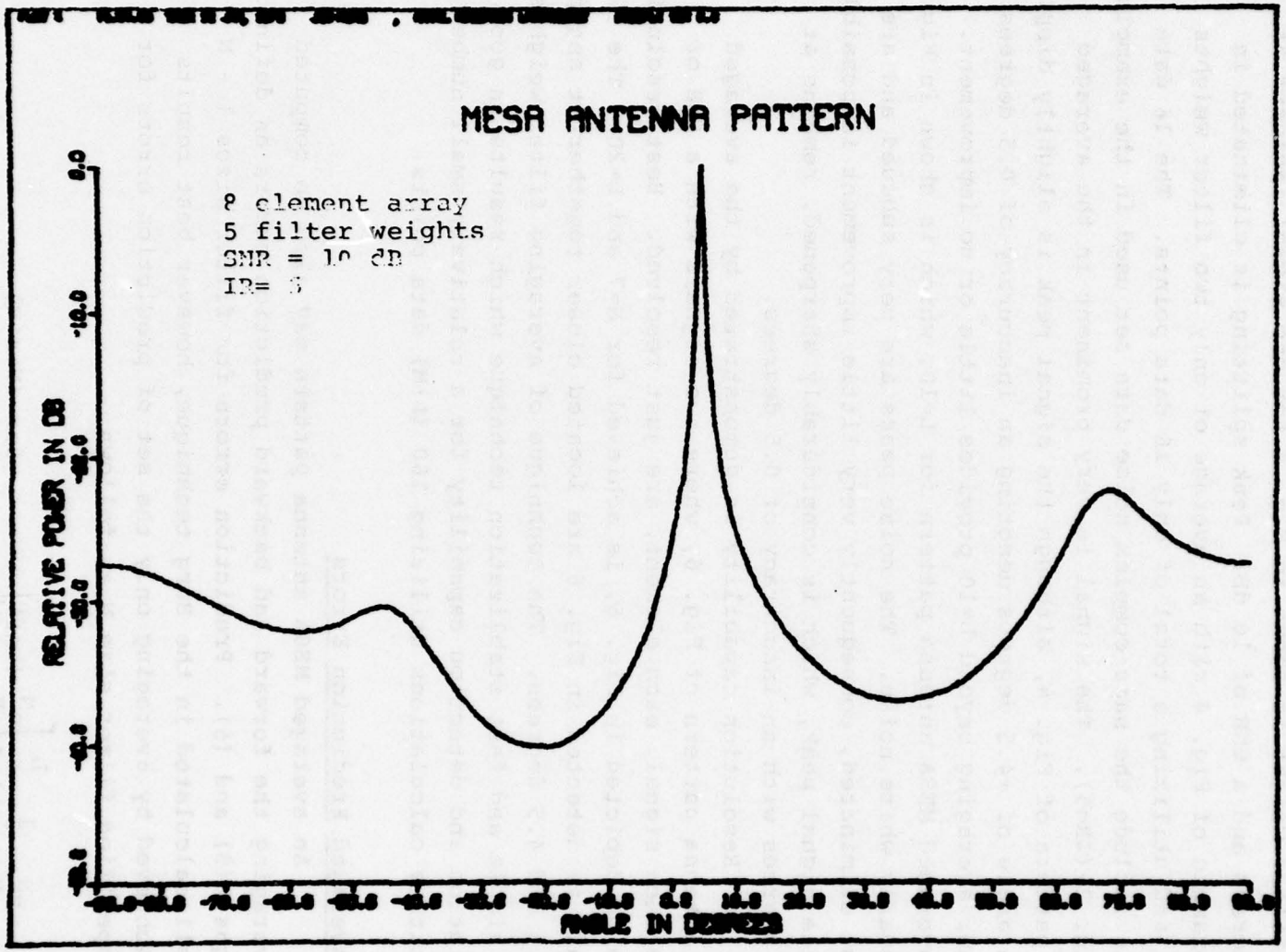

Fig. 4 - One signal, averaged filter weights, L=2

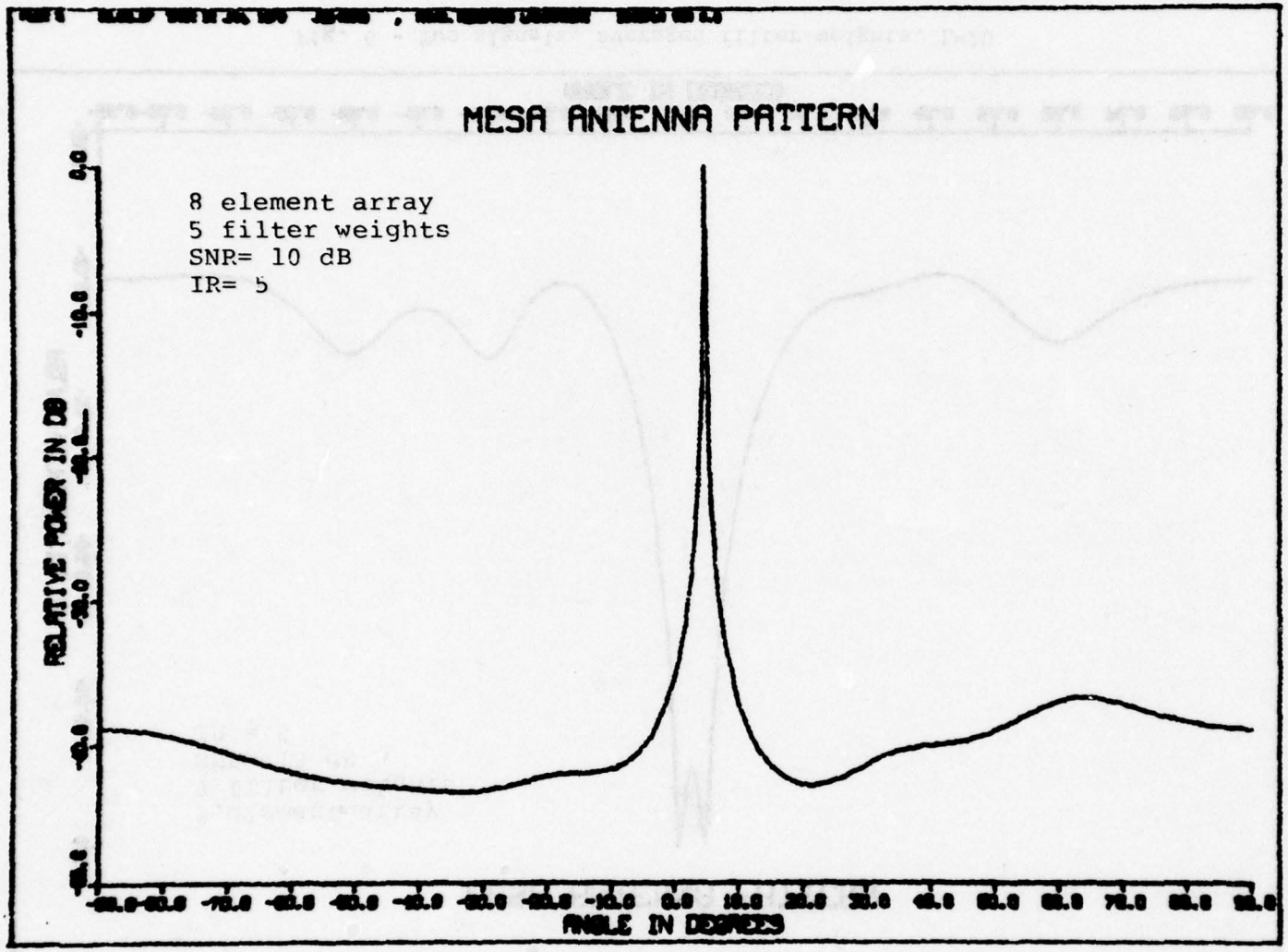

Fig. 5 - One signal, averaged filter weights, L=10

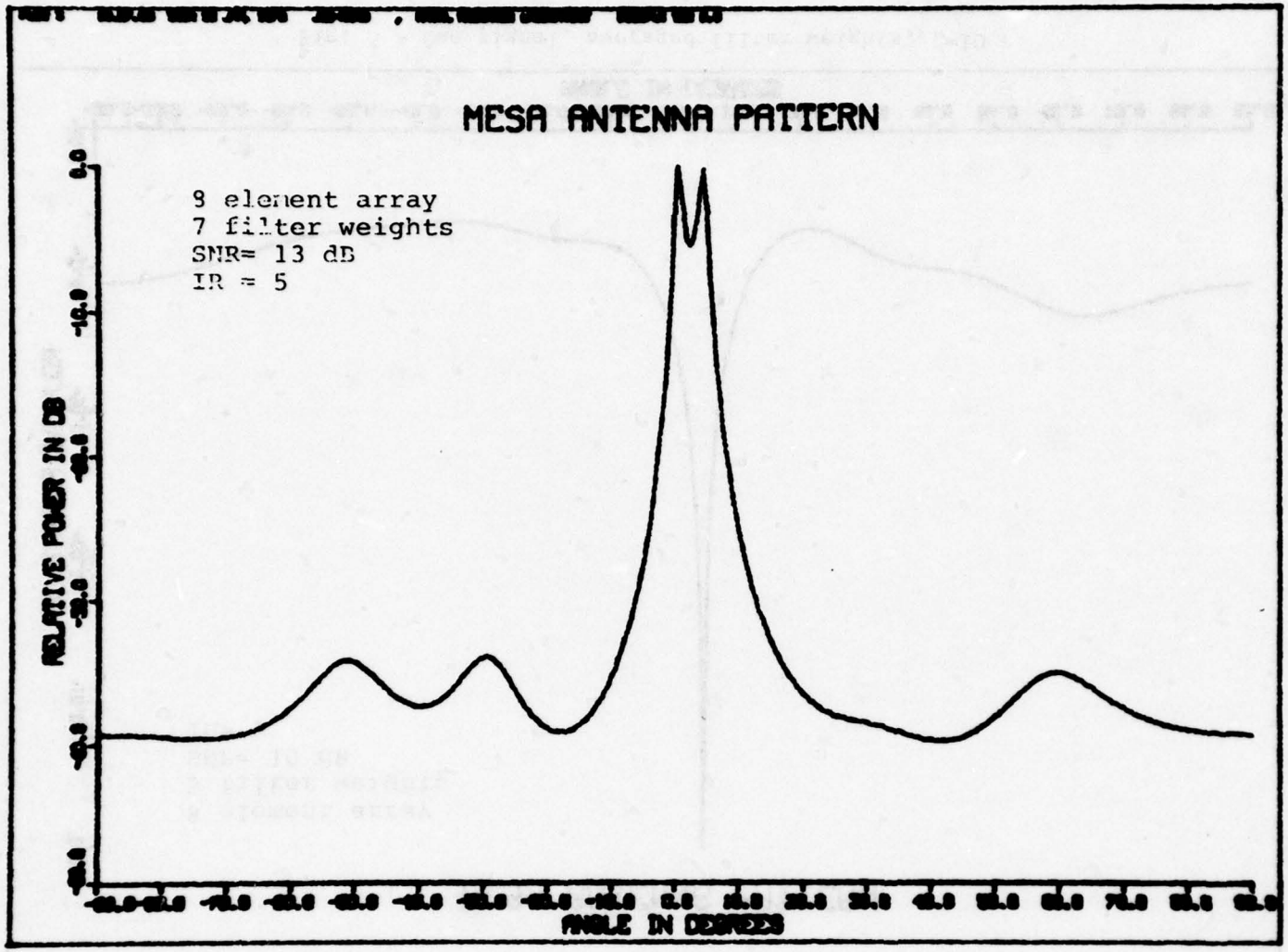

Fig. 6 - Two signals, averaged filter weights, L=20

$$B_n^N = \frac{1}{L} \sum_{k=1}^{L} \left[B_n^N \quad (k\Delta t) \right]_k \qquad \text{for } (1 \leq n \leq M-N)$$

Both prediction error averaging and filter weight averaging are comparatively simple and fast averaging techniques, but the two averaged antenna patterns are quite dissimilar.

An averaged MESA antenna pattern computed by averaging the prediction errors is shown in Fig. 7 where the split peak (obtained for L=1, Fig. 3) is eliminated by averaging with only one additional data set (L=2). The result of further averaging is shown for L=10 in Fig. 8. The filter size (N=5) and the complex data set for IR=5 are the same as used in all previous examples of averaged MESA patterns. It is evident by observation of Figs. 7 and 8 that averaging of prediction errors does not whiten the noise and does not enhance the SNR, but peak splitting is eliminated. In Fig. 8 the signal peak is located at +4 degrees for an error of one degree. Further averaging beyond L=10 does not improve the antenna pattern for one signal and an 8 element array.

Prediction errors are averaged in Fig. 9 for two signals incident at 0 and +6 degrees. The two signals are well resolved and the SNR is improved for L=30. One signal is accurately located at 0 degrees, while the second signal which is located at +4.5 degrees is in error by 1.5 degrees. The SNR is significantly improved, more so than for the single signal of Figs. 7 and 8.

C. Averaged Covariance Matrix

While not so obvious, the equations of the Burg technique do contain elements of the covariance matrix. These elements may be averaged and incorporated into the Burg technique equations without altering the utilization or the characteristics of the Burg technique. The only independent filter weight Γ_{N+1}^{N+1}, which is defined by eqn. (4) of the Burg technique, is a function of the forward and backward prediction errors, F_{N+I}^N and B_I^N .

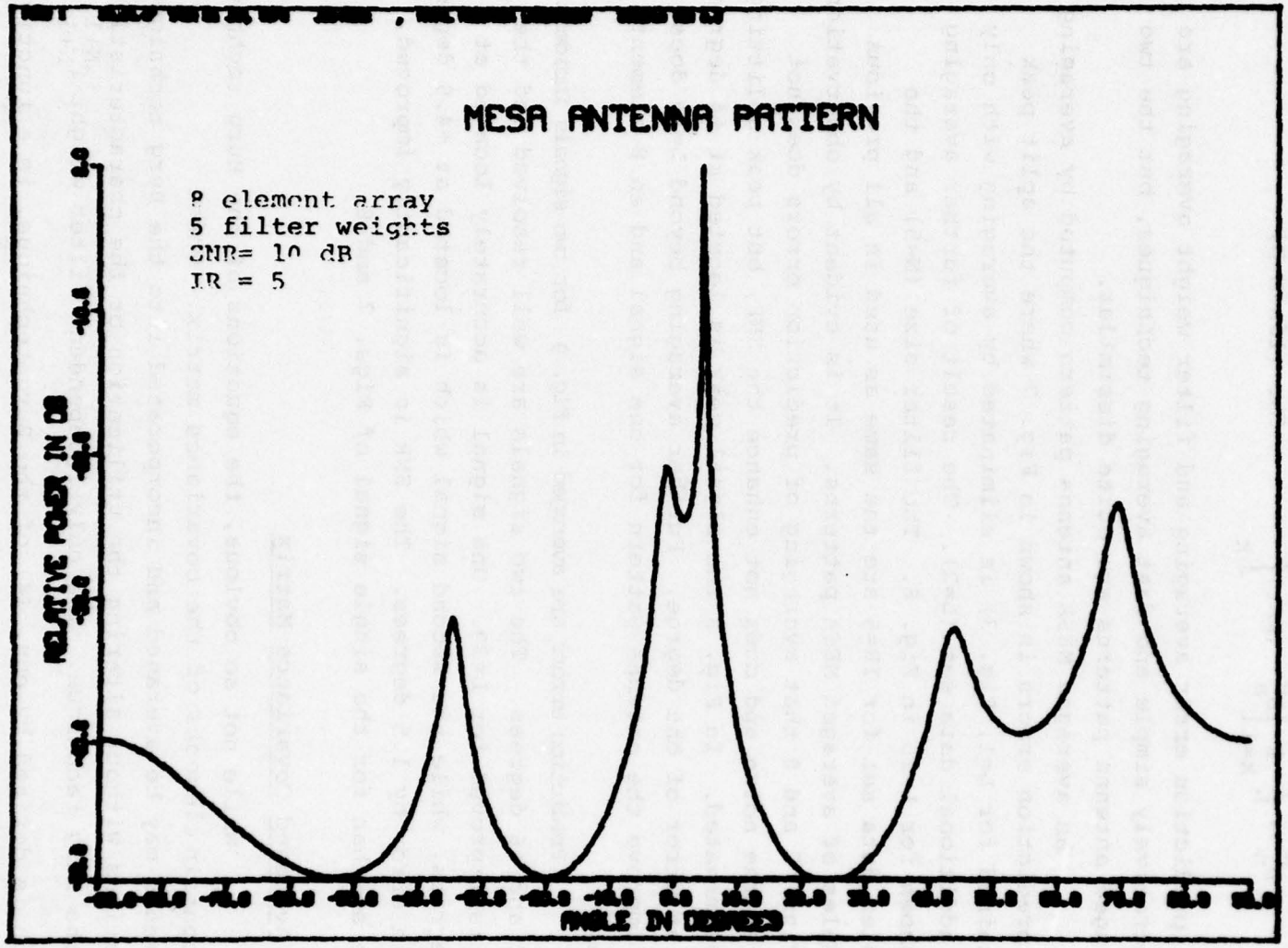

Fig. 7 - One signal, averaged prediction errors, L=2

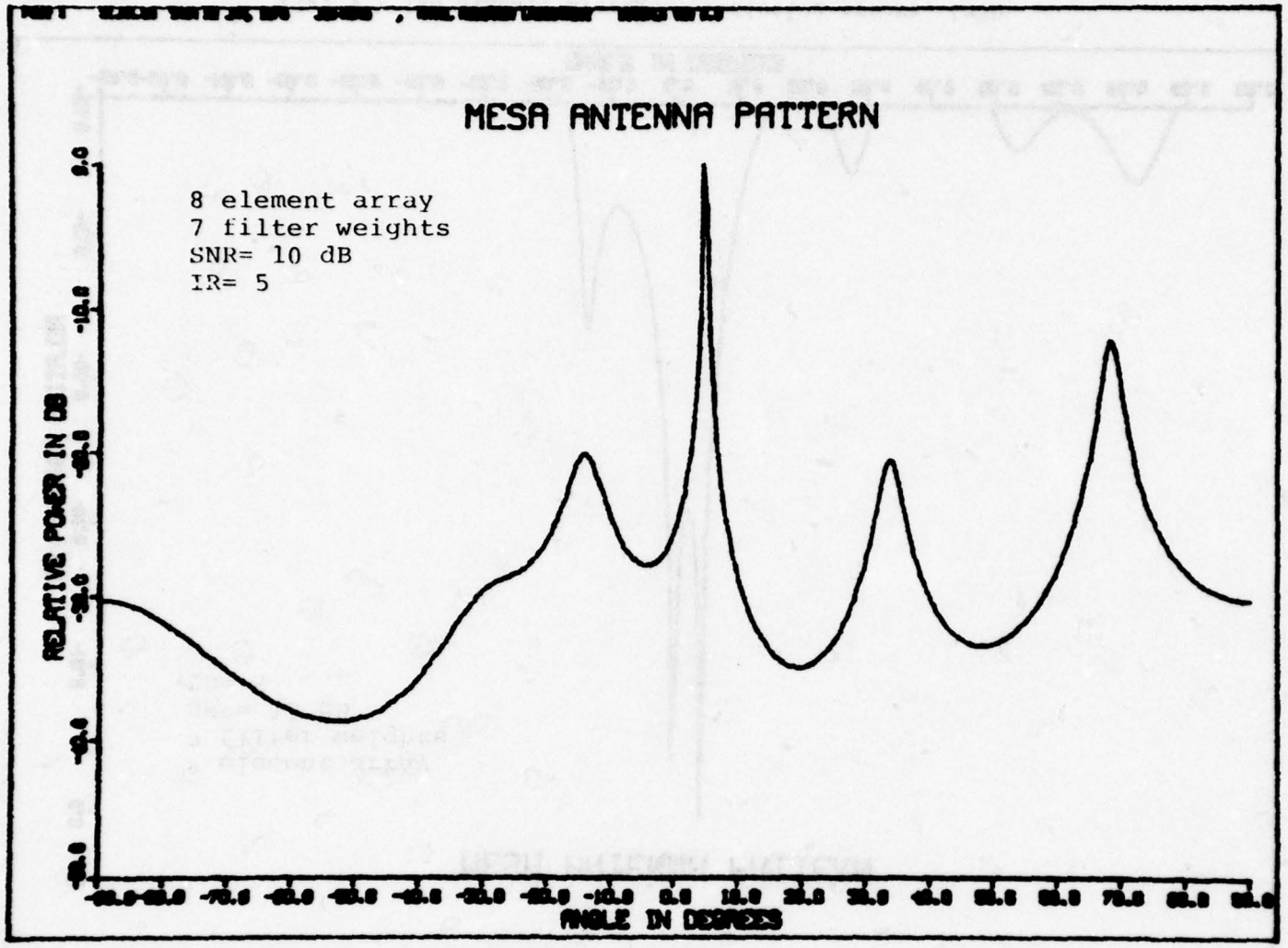

Fig. 8 - One signal, averaged prediction errors, L=10

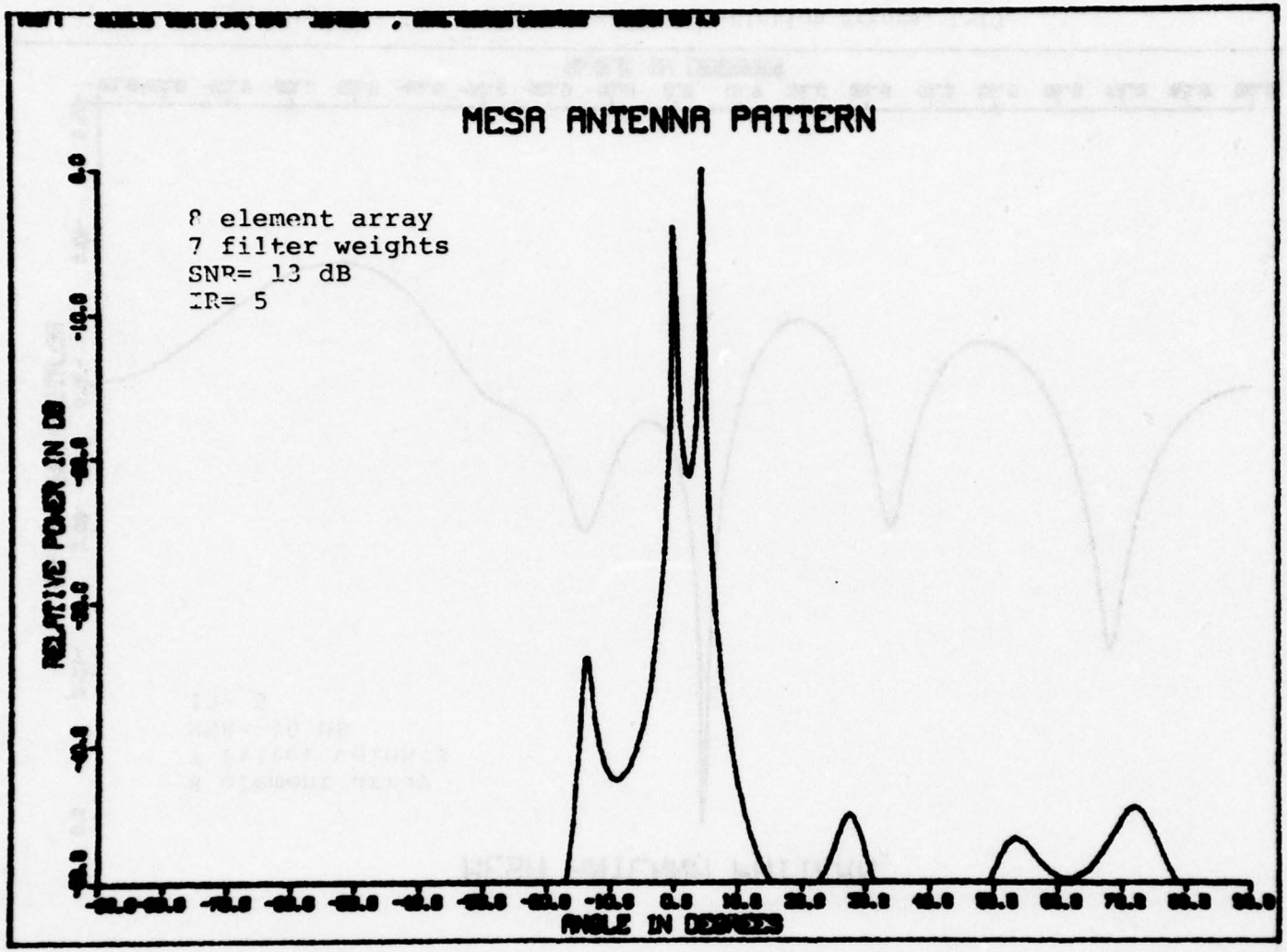

Fig. 9 - Two signal, averaged prediction errors, L=30

Products of the prediction errors may be considered as functions of the covariance matrix elements by considering the original definition as follows:

Forward prediction error

$$F_{N+I}^{N} = \sum_{n=1}^{N} \gamma_n^N \, X_{n+I-n+1} \tag{7}$$

Backward prediction error

$$B_I^N = \sum_{n=1}^{N} (\gamma_n^N)^* \, X_{I+n-1} \tag{8}$$

where $\gamma_1^N = 1.0$

The last filter weight γ_{N+1}^{N+1} of eqn. (4) may be expressed as the ratio of two functions, TOP and BOTM, as follows:

$$\gamma_{N+1}^{N+1} = -2 \; \text{TOP/BOTM}$$

where

$$\text{TOP} = \sum_{I=1}^{M-N} F_{N+I}^{N} \, (B_I^N)^* \tag{9}$$

$$\text{BOTM} = \sum_{I=1}^{M-N} \left[(F_{N+I}^{N})^2 + (B_I^N)^2 \right] \tag{10}$$

Insertion of the prediction error definitions eqns. (7) and (8) into eqns. (9) and (10) and re-ordering the summations yields the desired functional form as follows:

$$\text{TOP} = \sum_{I=1}^{M-N} \left[\sum_{M=1}^{N} \gamma_M^N \, X_{N+I-m+1} \sum_{n=1}^{N} \left((\gamma_n^N)^* \, X_{I+n-1} \right)^* \right]$$

$$TOP = \sum_{m=1}^{N} \sum_{n=1}^{N} \gamma_m^N \gamma_n^N \; r\,(N-M-n+2)$$

where

$$r\,(N-m-n+2) = \sum_{I=1}^{M-N} X_{I+N-m+1} \; X^*_{I+n-1} \tag{11}$$

$$BOTM = \sum_{I=1}^{M-N} \left[\sum_{m=1}^{N} \gamma_m^N \, X_{I+N-m+1} \sum_{n=1}^{N} (\gamma_n^N)^* \, X^*_{N+I-n+1} \right.$$

$$\left. + \sum_{m=1}^{N} (\gamma_m^N)^* \, X_{N+m-1} \sum_{n=1}^{N} \left((\gamma_n^N)^* \, X_{I+n-1} \right)^* \right]$$

$$BOTM = \sum_{m=1}^{N} \sum_{n=1}^{N} \gamma_m^N \, (\gamma_n^N)^* \, r(n-m) + \sum_{m=1}^{N} \sum_{n=1}^{N} (\gamma_m^N)^* \, \gamma_n^N \, r(m-n)$$

where

$$r(n-m) = \sum_{I=1}^{M-N} X_{N+I-m+1} \; X^*_{N+I-n+1} \tag{12}$$

$$r(m-n) = \sum_{I=1}^{M-N} X_{I+m-1} \; X^*_{I+n-1} \tag{13}$$

It is apparent that the autocorrelation coefficients defined by eqns. (11), (12) and (13) may be averaged as follows:

$$\bar{r}(N-m-n+2) = \sum_{I=1}^{M-N} \frac{1}{L} \sum_{k=1}^{L} X(k\Delta t)_{N+I-m+1} \; X^*(k\Delta t)_{I+n-1} \tag{14}$$

$$\bar{r}\ (m-n) = \sum_{I=1}^{M-N} \frac{1}{L} \sum_{k=1}^{L} X(k\Delta t)_{N+I-m+1}\ X^{*}(k\Delta t)_{N+I-n+1} \qquad (15)$$

$$\bar{r}(m-n) = \sum_{I=1}^{M-N} \frac{1}{L} \sum_{k=1}^{L} X(k\Delta t)_{I+m-1}\ X^{*}(k\Delta t)_{I+n-1} \qquad (16)$$

The autocorrelation coefficients (eqns. (11), (12) and (13)) are elements of the covariance matrix for the data set $X_1, X_2, \ldots X_M$. The averaged covariance matrix elements given by eqns (14), (15) and (16) may be utilized to compute the last filter weight Γ_{N+1}^{N+1} and an averaged MESA antenna pattern.

The results due to averaging of the covariance matrix are observed in Fig. 10 where the split peak shown in Fig. 3 is eliminated with only one additional data set (L=2). Also the noise is considerably whiter which greatly improves the SNR. Further averaging provides little additional improvement as noted by Fig. 11, where for L=10 the noise appears slightly whiter and the SNR is slightly enhanced over the results shown in Fig. 10.

Two signals located at 0 and +6 degrees are well resolved in Fig. 12 with covariance matrix averaging, for L=10 and an input SNR of 13 dB each signal. The background noise is substantially reduced although it is not as white as the noise that appears in Fig. 11. Averaging of the covariance matrix elements is, as demonstrated, an excellent averaging and stablization technique.

D. Averaged MESA Snapshots

Individual MESA antenna patterns, which are referred to as "snapshots" (e.g. Fig. 1a, 1b), may be averaged in order to obtain a stable antenna pattern. This method has been utilized (14) successfully using optimal filter sizes. However, if the optimal filter size cannot be determined, a fixed filter size may be selected

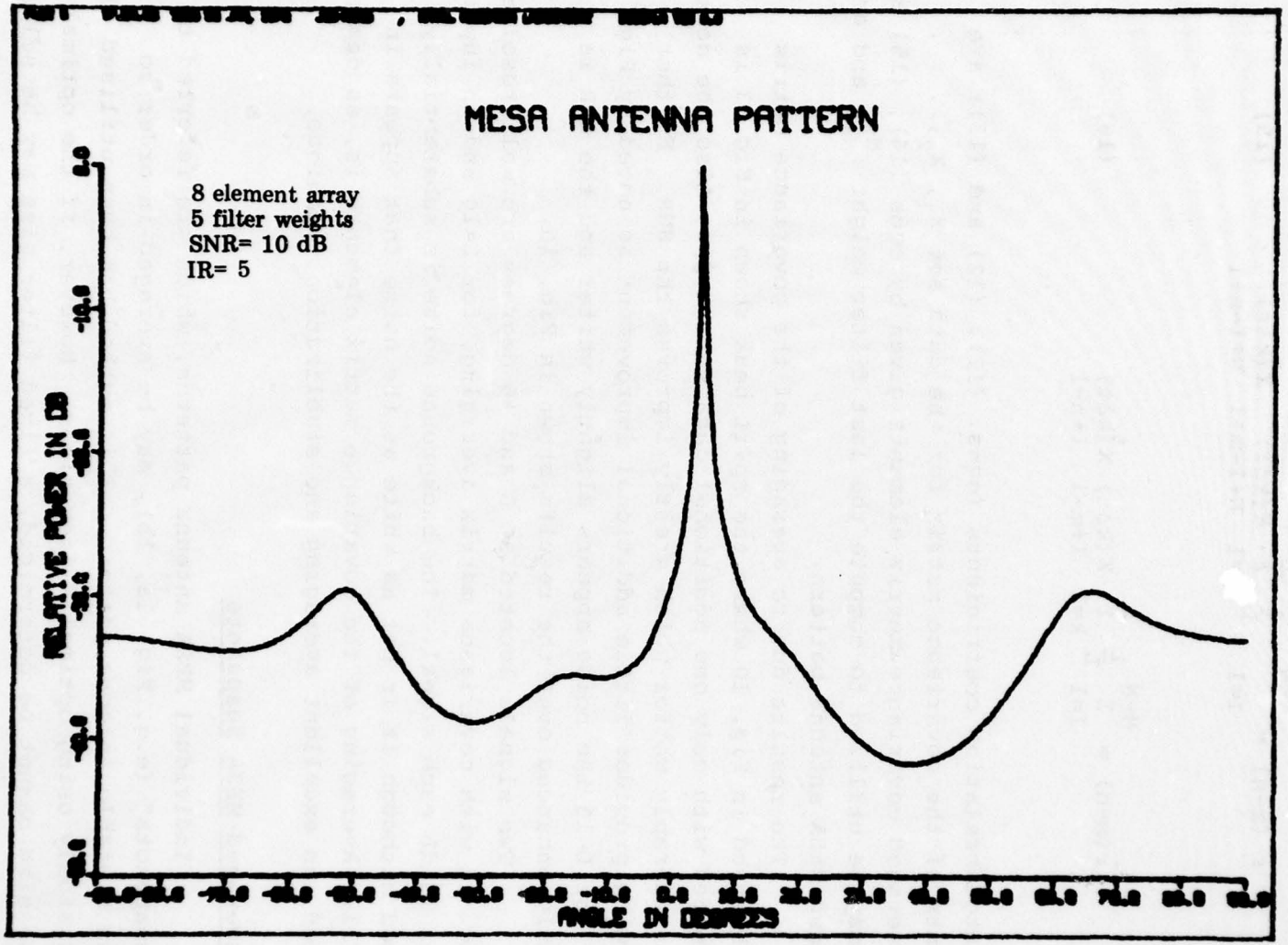

Fig. 10 - One signal, averaged covariance matrix, L=2

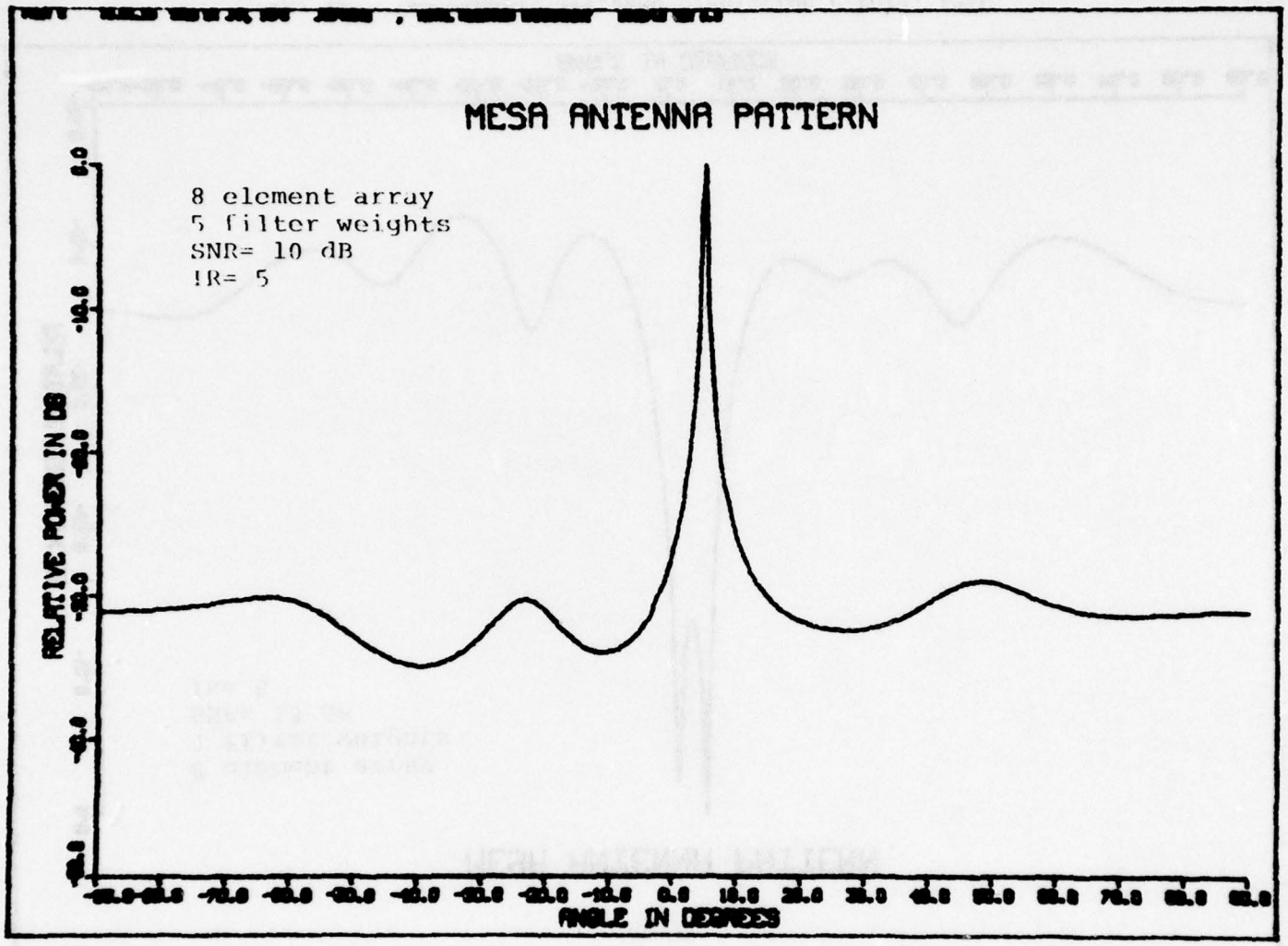

Fig. 11 - One signal, averaged prediction errors, L=10

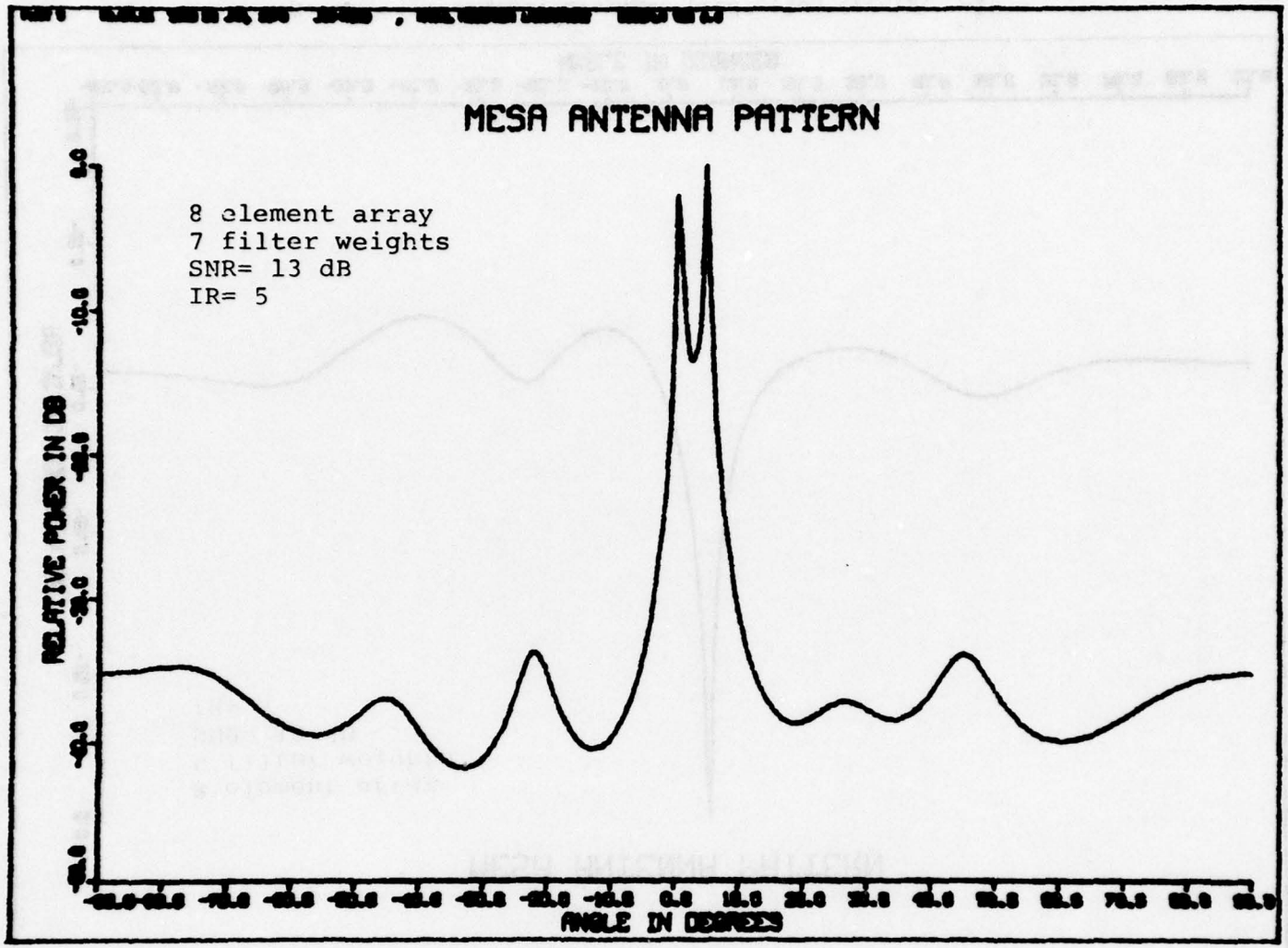

Fig. 12 - Two signal, averaged prediction errors, L=10

for computing all the individual MESA snapshot antenna patterns. The best resolution is always achieved using the largest possible filter size (N=M-1). However, the larger filter sizes are also the most unstable. Consequently, while an average of many MESA snapshots improves stability, the resultant stable pattern may not be a very accurate antenna pattern.

Averaging results for two filter sizes (N=5 and N=7) are demonstrated in the three following examples. A simple average of two MESA snapshots (L=2) is shown in Fig. 13 for one signal incident at 5 degrees with a SNR of 10 dB. The split peak that occurs for L=1 (Fig. 3) is still present in the average of two snapshots. However, there is improvement in the SNR. There are of course twice the number of peaks (10) as expected for two MESA snapshots having five filter weights (N=5) each. The consequence of further averaging is demonstrated in Fig. 14 where 30 antenna patterns (computed for a signal incident at 5 degrees with a SNR of 10 dB) are averaged. There is further improvement in the signal peak definition and accuracy; the signal is located at +4 degrees, for an error of one degree. The SNR is improved substantially.

In Fig. 15 the resultant average of MESA antenna patterns for two signals incident at 0 and +6 degrees is disappointing as the two signal peaks are not very well defined. Instead there are four strong peaks, two of which are in error. There is of course improvement in the SNR, but the resolution characteristics are very poor. In the example of Fig. 15, averaged MESA snapshots all have the maximum number (7) of filter weights. Better results have been achieved (14) using an optimal filter size, however the optimal filter size can only be computed if the incident signal angles are known.

VI. ADAPTIVE FILTER WEIGHTS

While the MESA technique is inherently adaptive, other adaptive methods which have been demonstrated (17, 18) have simple procedures for updating the filter weights. One such procedure (12)

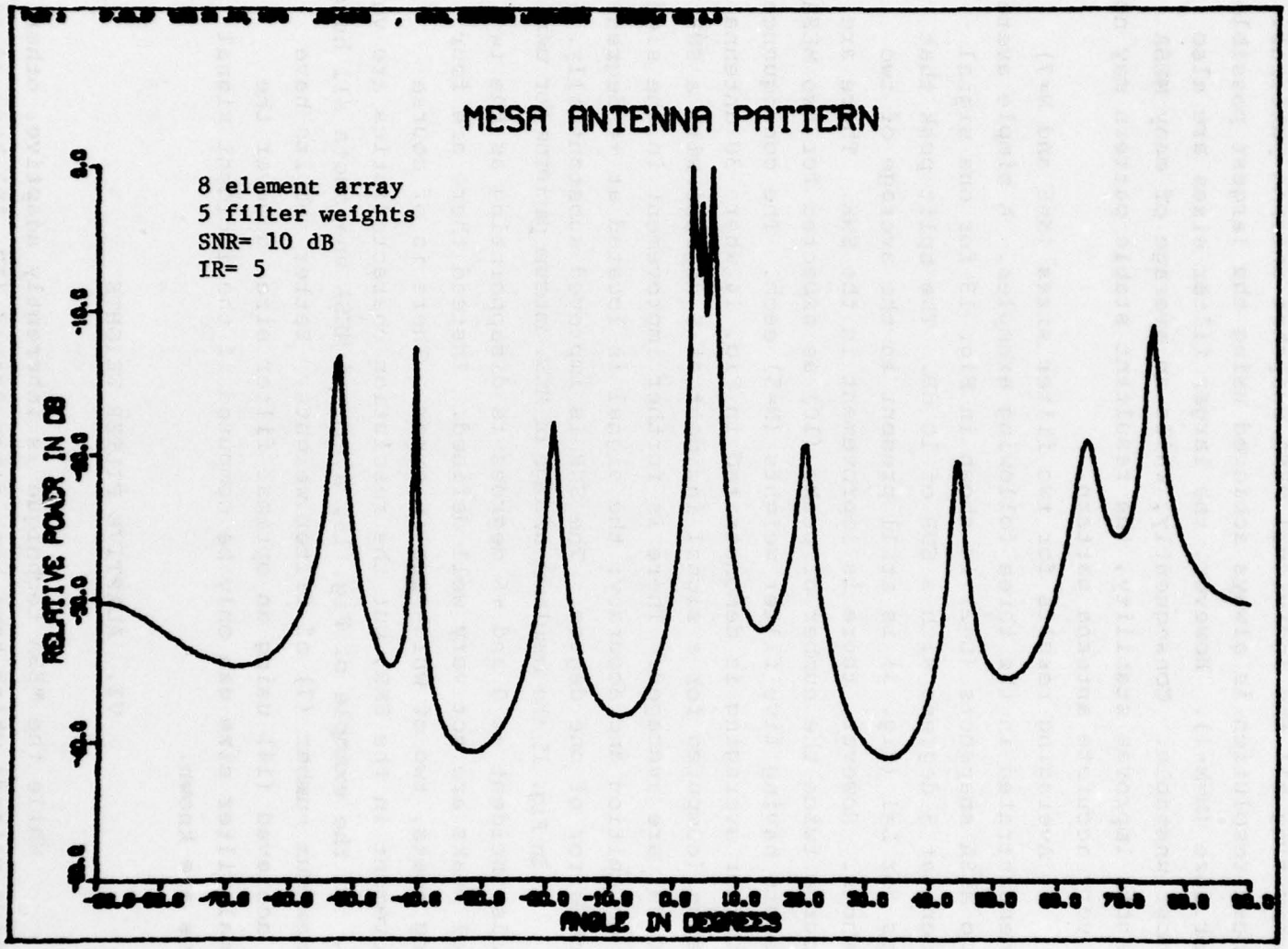

Fig. 13 - One signal, averaged patterns, L=2

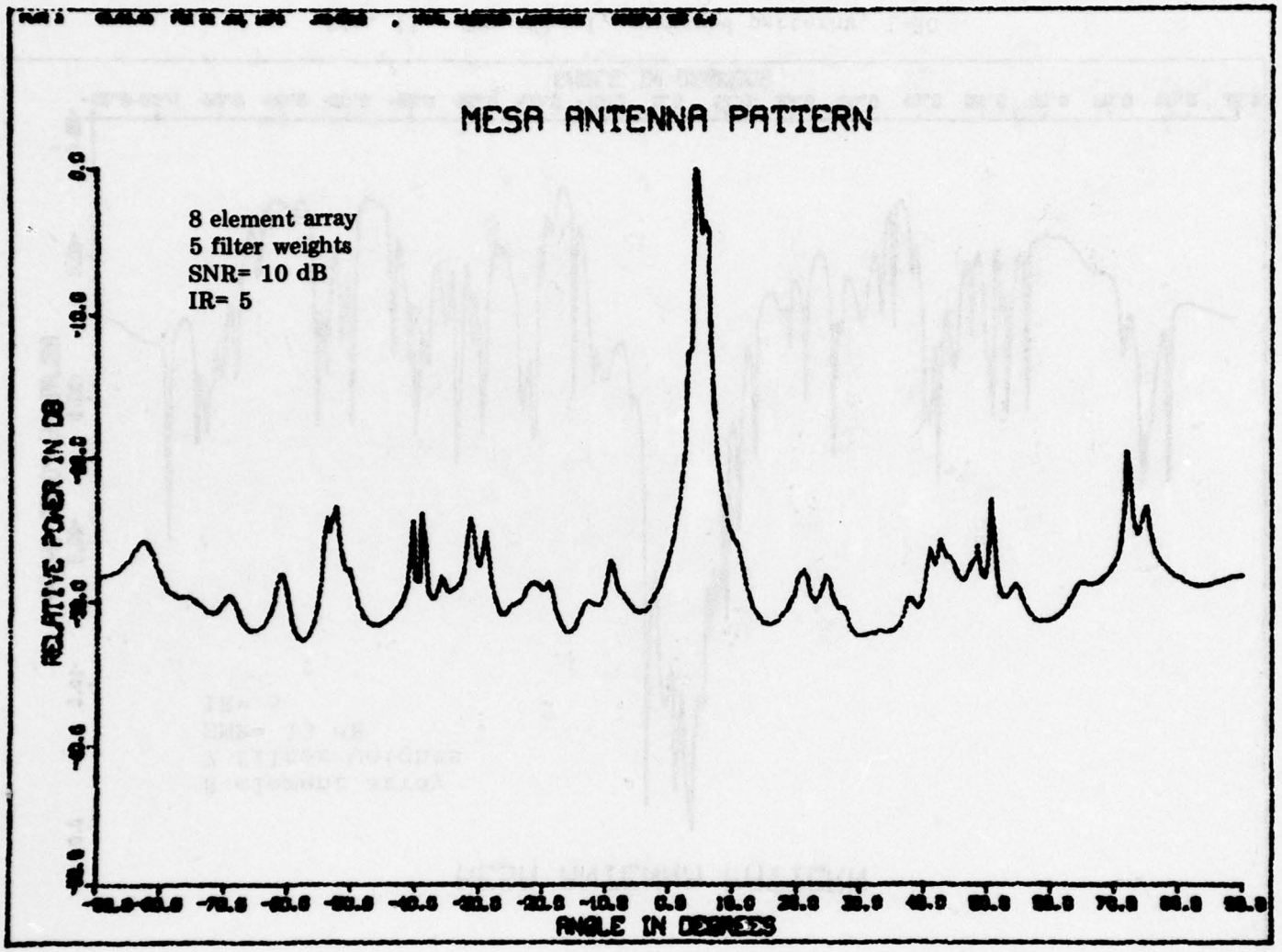

Fig. 14 - One signal, averaged patterns, L=30

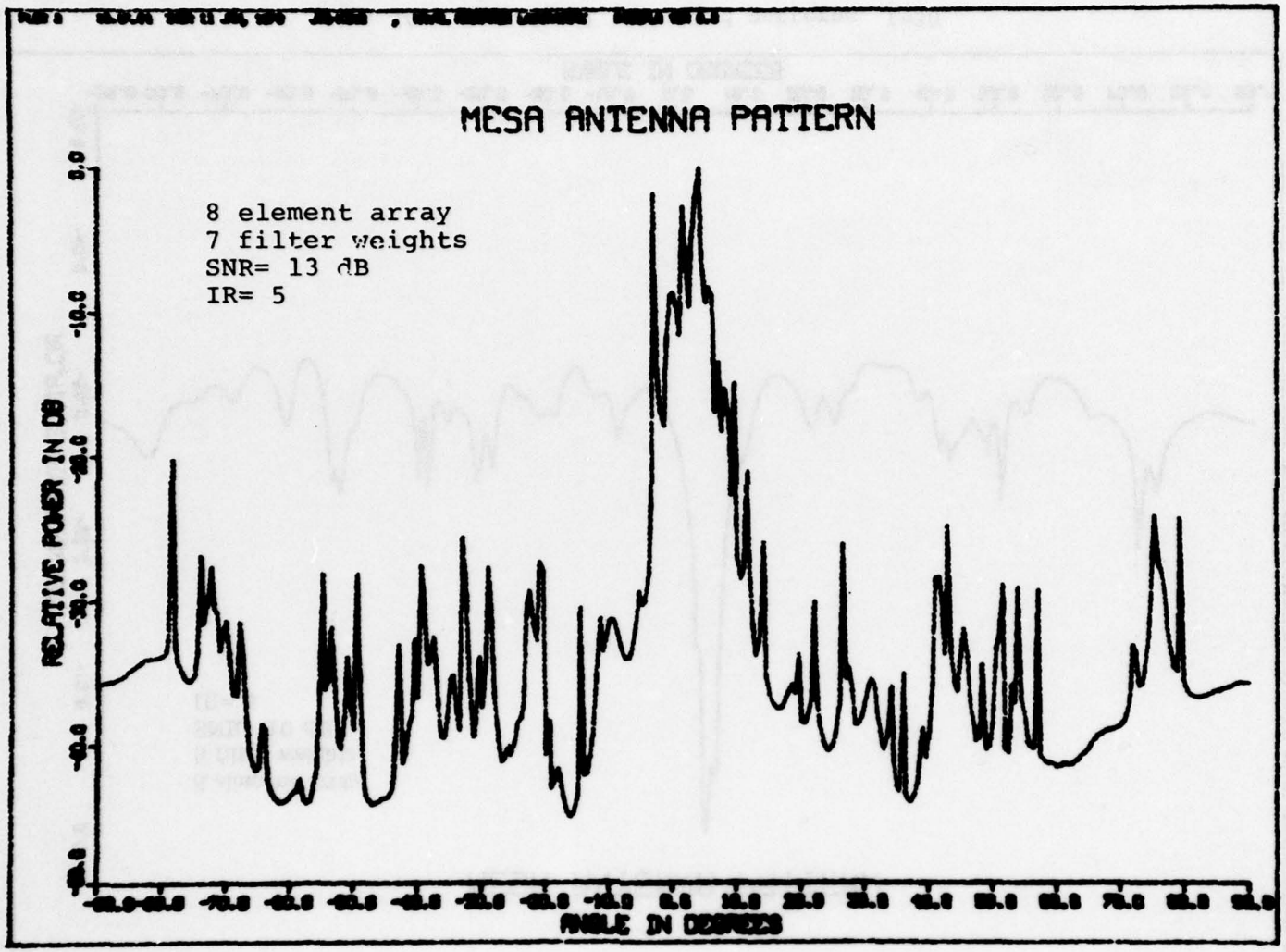

Fig. 15 - Two signal, averaged patterns, L=30

increases the filter weights in proportion to the correlation of the prediction error with the data set. For example, a filter weight W(k) computed at time $k\Delta t$ may be updated at a later time $(k+1)\Delta t$ to give W(k+1) as follows:

$$W(k+1) = W(k) + \mu \sum_{n=1}^{M} e_n(k) X_n^*(k) \qquad (17)$$

where the correlation is taken over all computed prediction errors $e_n(k)$. The prediction errors are defined as follows:

$$e_n(k) = X_n(k) - \hat{X}_n(k) \qquad (18)$$

for data samples $X_n(k)$ and predicted values $\hat{X}_n(k)$. The proportionality constant is denoted by the convergence parameter μ.

In order to incoporate this procedure into the MESA technique, a first set of filter weights is computed in the usual manner as defined by eqns. (3) and (4). Subsequent filter weights $\Gamma_n^N(k+1)$ may then be computed according to eqn. (17) as follows:

$$\Gamma_n^N(k+1) = \Gamma_n^N(k) + \mu \sum_{n=1}^{M-N} e_n^N(k) X_n^*(k) \qquad (19)$$

where the prediction error is actually the sum of the forward and backward prediction errors over all possible (M-N) errors as follows:

$$e_n^N(k) = F_{n+N}^N(k) + B_n^N(k) \qquad (20)$$

However, with use of the Burg technique, only the last filter weight Γ_N^N, need be computed with eqn. (19), since all other filter weights

($n<N$) are dependent upon Γ_N^N according to eqn. (3).

As the prediction error is whitened, the additive adaptive component is reduced, since the correlation of a whiter prediction error with the data set is smaller. Consequently, the adaptive filter weights may converge to become a whitening filter.

The result of updating MESA filter weights is illustrated in Fig. 16 where an "adapted" MESA antenna pattern is hown for one signal incident at +5 degrees, SNR=10 dB, and L=2. The "adapted" pattern for L=2 is of course quite similar to the computed MESA snapshot (L=1) shown in Fig. 3, since the filter weights have been modified only once. The split peak is still present for L=2 in Fig. 16, but with further adaption the split peak is eliminated as shown in Fig. 17 for L=10. However, the SNR is not improved, although three noise peaks have been reduced. As observed in Fog. 17 the noise has remained peaked even after ten adaptions. Obviously the adaption method does not tend to whiten the noise, and consequently the results are most disappointing.

In another application of the adaptive method, two signals incident at 0 and +6 degrees are resolved in ten adaptions (L=10) as shown in Fig. 18, where the SNR is 13 dB for each signal. One signal is located accurately at +6 degrees while the other signal is located at +1.5 degrees with an error of 1.5 degrees. The SNR is improved with respect to the original (L=1) MESA snapshot of Fig. 3. However, the noise is not whitened in the adaptive process as had been anticipated.

The results from using adaptive filter weights with MESA are very disappointing, and in addition the value of a convergence parameter must be specified. In the three preceding examples of the adaptive technique the value of the convergence parameter μ is quite critica. If μ is too small, there is little improvement in the computed antenna pattern, and if μ is too large, there may be considerable distortion of the signal peak.

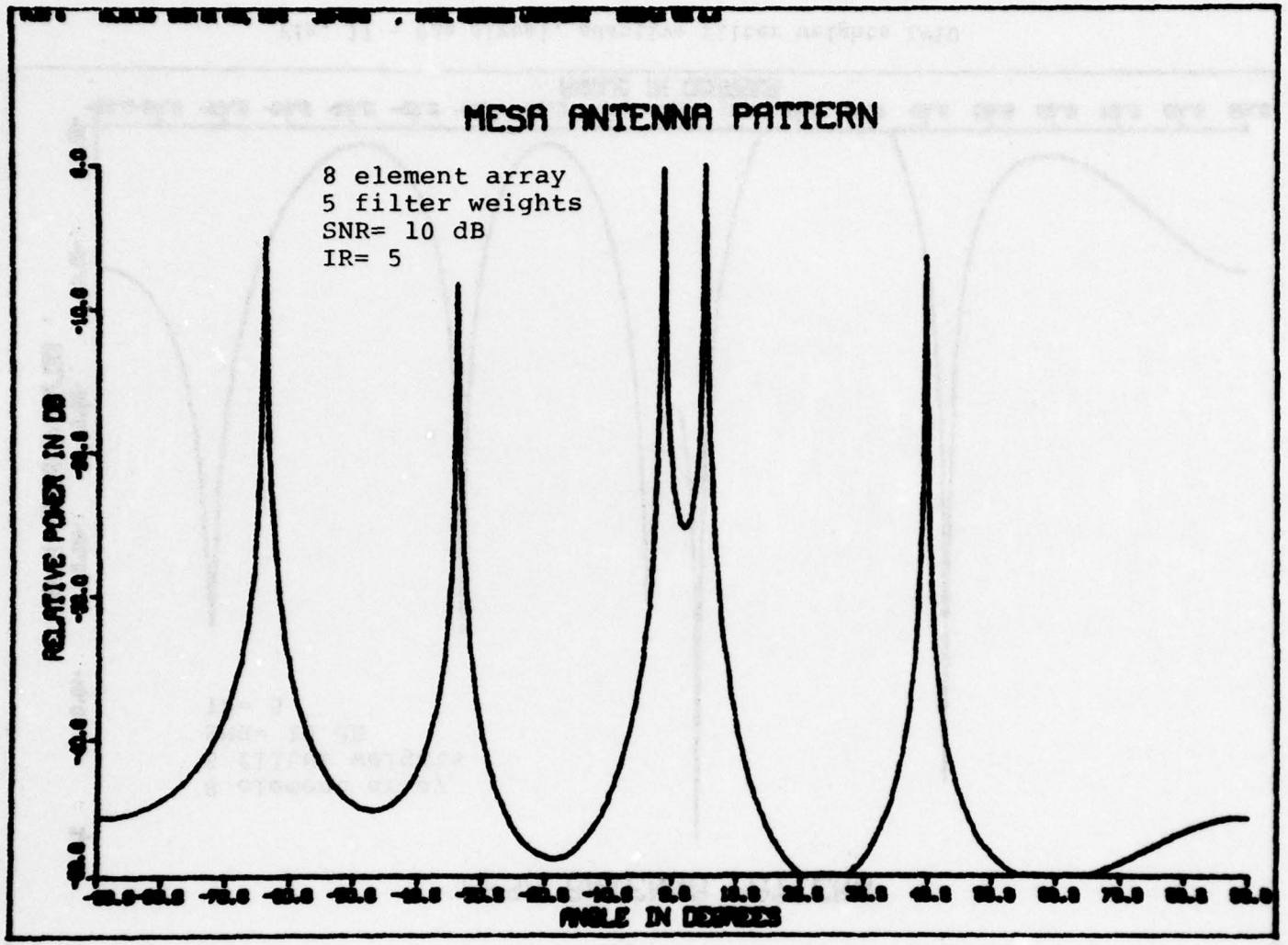

Fig. 16 - One signal, adaptive filter weights, L=2

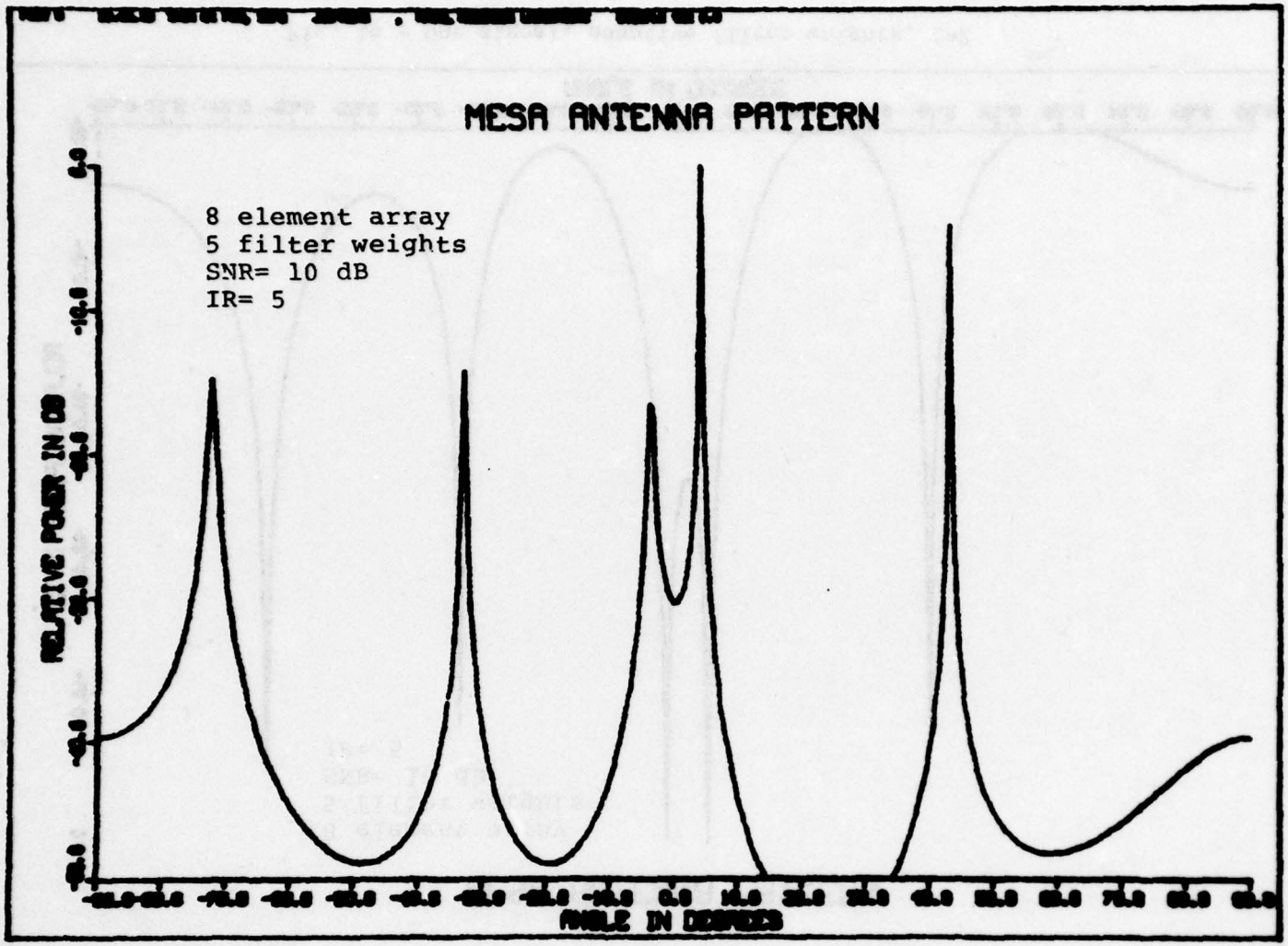

Fig. 17 - One signal, adaptive filter weights L=10

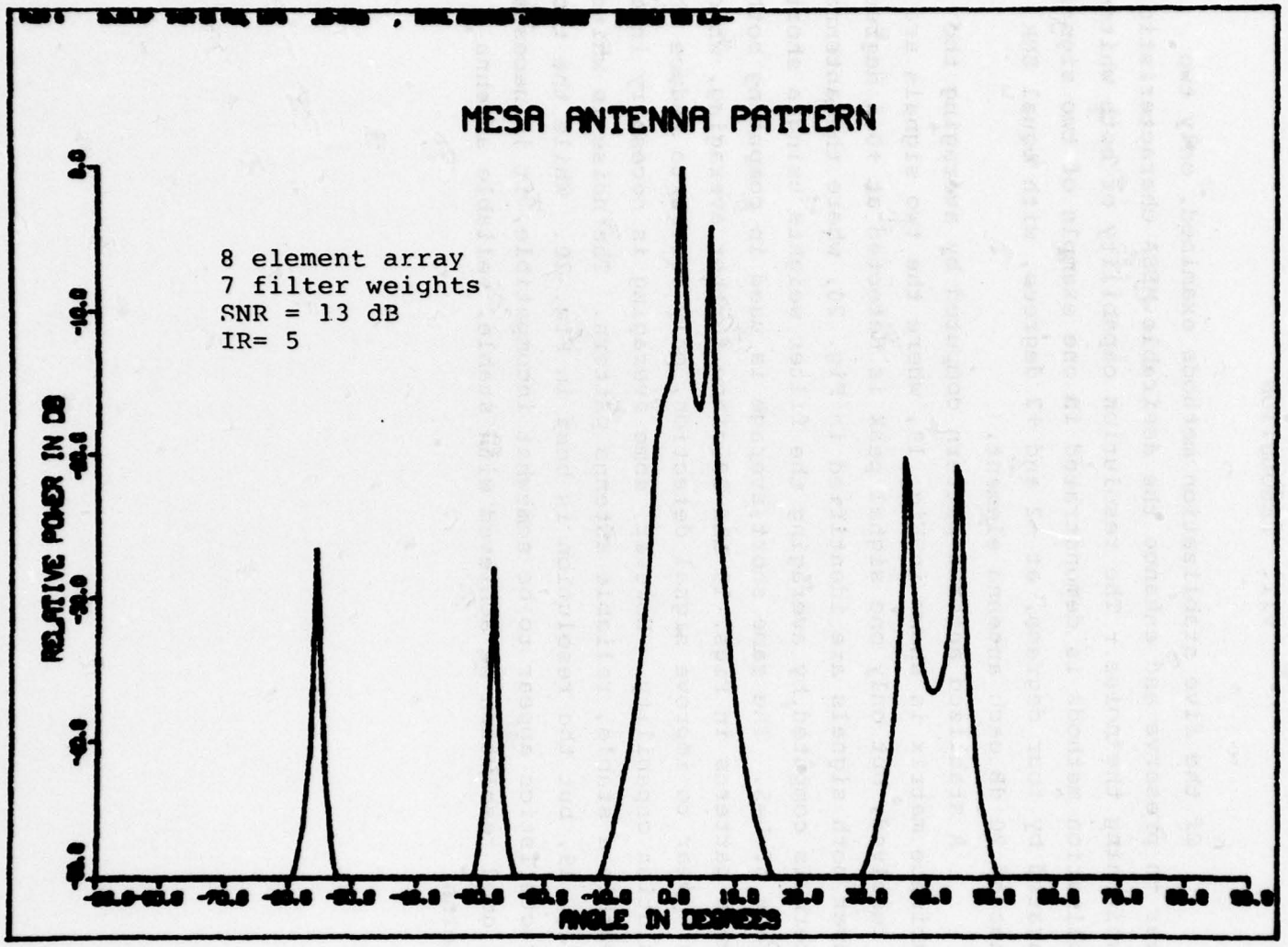

Fig. 18 - Two signals, adaptive filter weights, L=10

VII. RESOLUTION

Of the five stablization methods examined, only two appear to preserve and enhance the desirable MESA characteristic of whitening the noise. The resolution capability of both whitening, stablization methods is demonstrated in one example of two signals separated by four degrees, at -2 and +2 degrees, with equal SNR values of 20 dB each antenna element.

A stablized antenna pattern computed by averaging the covariance matrix is shown in Fig. 19, where the two signals are not resolved, but only one signal peak is detected at +0.5 degrees. However both signals are identified in Fig. 20, where the antenna pattern is computed by averaging the filter weights using a short average of L=5. The same short average is used in computing both antenna patterns in Figs. 19 and 20 since further averaging, which does appear to improve signal detection, only serves to reduce the resolution capability. However, some averaging is necessary in order to obtain a stable, reliable antenna pattern. The noise is whiter in Fig. 19, but the resolution is best in Fig. 20. While the two characteristics appear to be somewhat incompatible, it is necessary that good resolution be achieved with stable, reliable antenna patterns.

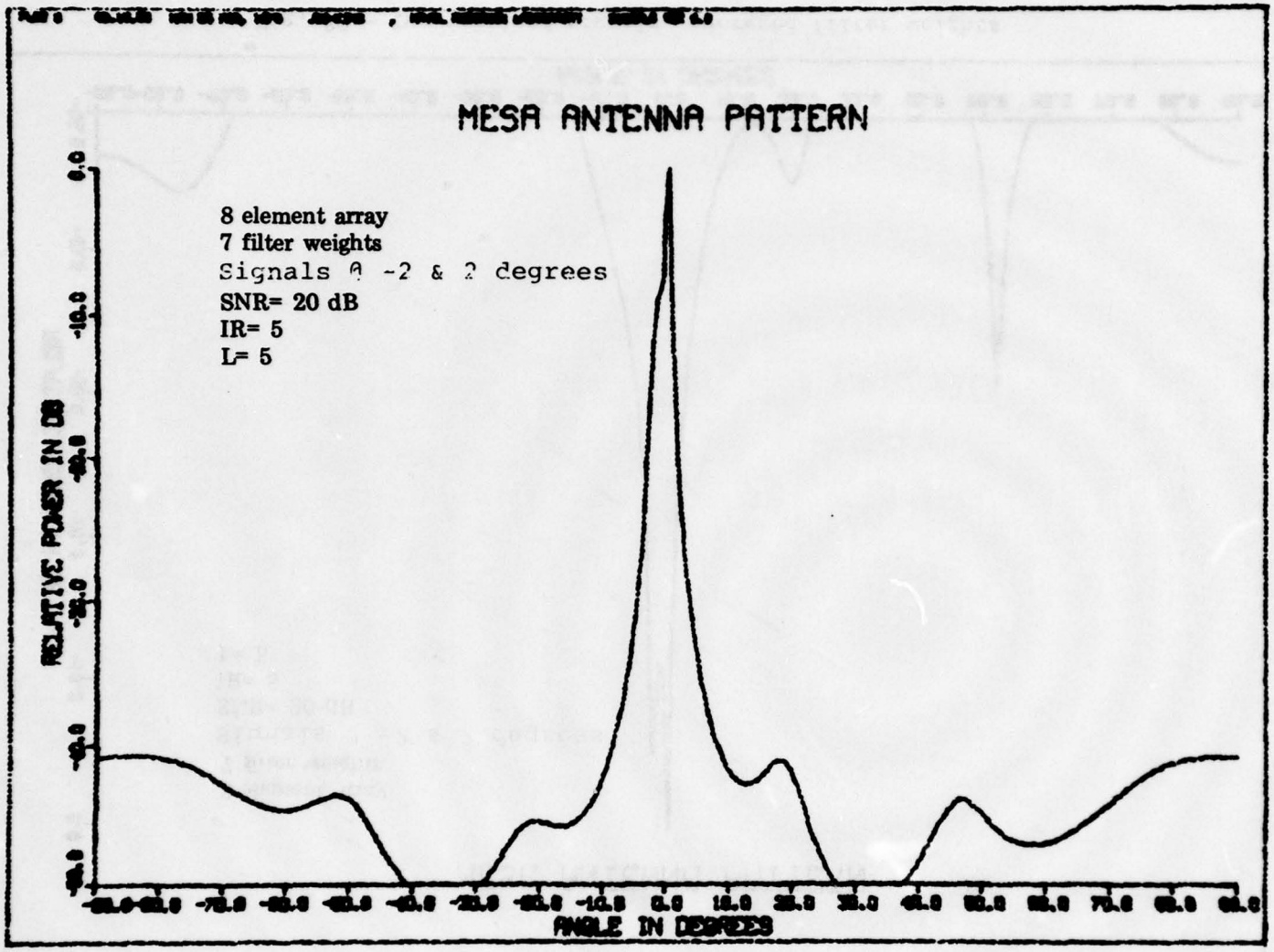

Fig. 19 - Two unresolved signals, averaged covariance matrix

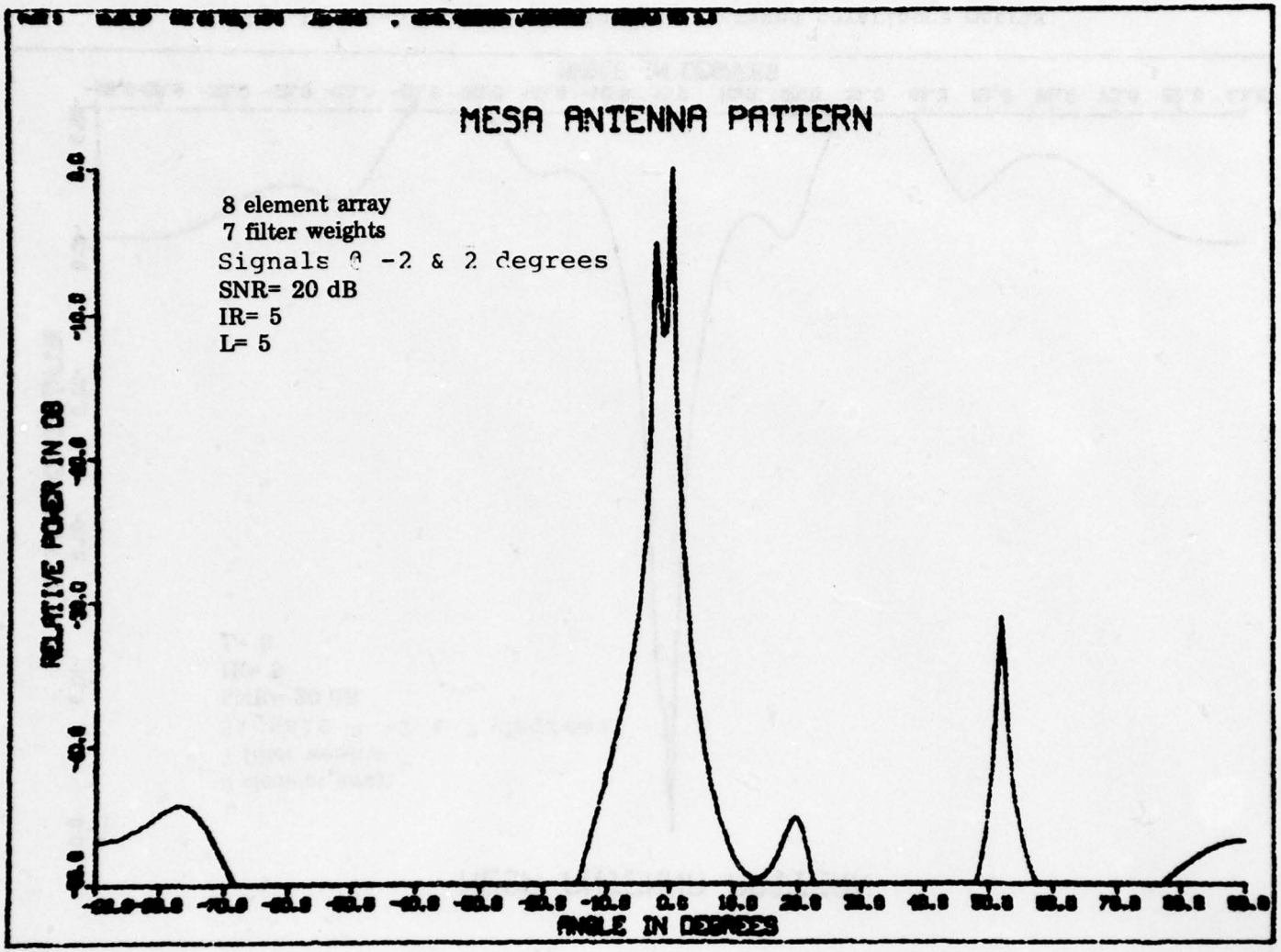

Fig. 20 - Two resolved signals, averaged filter weights

VIII. CONCLUSIONS

Split signal peaks, which are a common occurence in MESA snapshot patterns, are shown to be a consequence of noise interference. Such noise interference is virtually eliminated with use of the proposed stablization methods.

Of the five stablization techniques examined, two have excellent characteristics, one other is only somewhat satisfactory, and two were very disappointing. An average of filter weights and an average of the covariance matrix are both very useful stablization methods. Both methods serve to whiten the noise and greatly improve the SNR. In addition, split signal peaks were not observed with use of either averaged filter weights or averaged covariance matrix elements. Further testing of these two averaging methods is clearly justified. Hopefully, resolution and SNR properties of these two excellent averaging and stablization techniques will be specifically determined in future research efforts.

It is doubtful that any of the other three examined stablization methods are worthy of further consideration. Neither the averaged prediction errors nor the adaptive filter weights served to whiten the noise, and the averaged MESA patterns proved to be most unstable.

In the one example of two signals separated four degrees the MESA antenna pattern computed by averaging filter weights provided the best signal resolution. However, many such examples need to be accumulated in order to determine the resolution characteristics of the recommended MESA stablization methods.

REFERENCES

1. Burg, John P., (1975), "Maximum Entropy Spectral Analysis", Ph.D. Thesis, Stanford Univ., #75-25,499 Univ. Microfilms Intl., Ann Arbor, Mich.

2. Parzen, E., (1969), "Multiple Time Series Modeling", in Multivariate Analysis - II, edited by P. R. Kirshnaiah, pp. 389 - 409, Academic Press, New York

3. Box, G. E., and Jenkens, G. M., (1970), Time Series Analysis Forecasting and Control, Holden-Day, San Francisco, Calif.

4. Yule, G. U., (1927), "On a Method of Investigating Periodicities in Distrubed Series with Special References to Wolfers Sunspot Numbers", Phil. Trans. Roy. Soc. London, Ser. A, Vol. 226, pp. 267-298

5. Fisher, R. A. (1912), "On an Absolute Criterion for Fitting Frequency Curves", Messenger of Math, Vol. 41, p. 155

6. Makhoul, John (1975), "Linear Prediction: A Tutorial Review", Proc. IEEE, Vol. 63, No. 4, pp. 561 - 580, (April, 1975)

7. Nuttall, Albert H., (1976), "Spectral Analysis of a Univariate Process with Bad Data Points, Via Maximum Entropy and Linear Predictive Techniques", NUSC Tech. Rept. 5303, Naval Underwater Systems Center, New London, Conn.

8. Lacoss, R. T. (1971), "Data Adaptive Spectral Analysis Methods", Geophysics, Vol. 36, No. 4 (Aug. 1971), pp. 661 - 675

9. Gerchberg, R. W. (1974), "Super-resolution through Error Energy Reduction", Optica Acta, Vol. 21, No. 9 pp. 709-720 (1974).

10. Papoulis, Sept., (1975), "A New Algorithm in Spectral Analysis and Band Limited Extrapolation", IEEE Trans. on Circuits and Systems, CAS-22, No. 9, pp. 735-742 (1975)

11. Cadzow, James A., (1978, "Improved Spectral Estimation from Incomplete Sampled - Data Observations", RADC Spectrum Estimation Workshop, Griffiss Air Force Base, New York.

12. Widrow and Hoff, "Adaptive Switching Circuits", IRE 1960 WESCON Conv. Rec., Part 4, pp. 96 - 104.

13. Van den Bos, A. (1971) "Alternative Interpretation of Maximun Entropy Spectral Analysis", IEEE Trans. on Information Theory, IT-17, pp. 493 - 494.

14. King, W. R., (1979) "Maximun Entropy Wavenumber Analysis", submitted to NRL for publication, Jan. 1979. Naval Research Laboratory, Washington, D. C.

15. King, Swindell and O'Brien, (1974), "Final Report on Development of a Curvilinear Ray Theory Model and Maximum Entropy Spectral Analysis", Texas Instruments.

16. Fougere, Zawalick and Radoski, (1976), "Spontaneous Line Splitting in Maximum Entropy Power Spectrum Analysis", Physics of the Earth and Planetary Interiors, Vol. 12, pp. 201 - 207 (1976)

17. Griffiths, L. J. (1969), "A Simple Adaptive Algorithm for Real-Time Processing in Antenna Arrays", Proc. IEEEE, Vol. 57, No. 10, pp. 1696 - 1704 (Oct. 1969).

18. Applebaum, S. P., (1966), "Adaptive Arrays", Syracuse Univ. Res. Corp., Rept. SPL TR 66-1, (Aug. 1966).